Structure

Structure

Volume 19
Number 1
January 12, 2011

www.cellpress.com

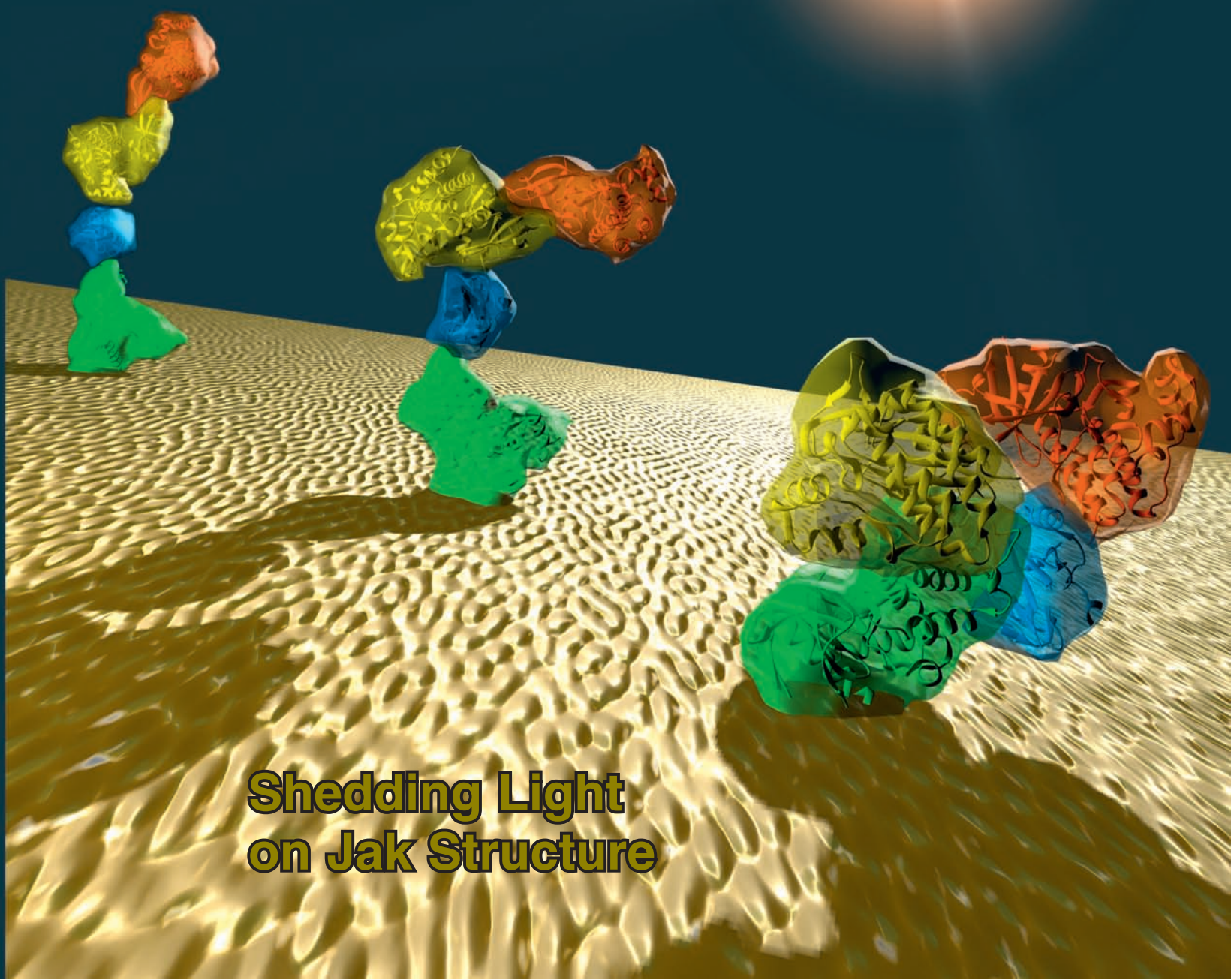

Shedding Light on Jak Structure

Structure Volume 19 Number 1 Pages 0000–0000 January 12, 2011

Structure
Article

Structural Snapshots of Full-Length Jak1, a Transmembrane gp130/IL-6/IL-6Rα Cytokine Receptor Complex, and the Receptor-Jak1 Holocomplex

Patrick J. Lupardus,[1,6] Georgios Skiniotis,[2,5,6] Amanda J. Rice,[2] Christoph Thomas,[1] Suzanne Fischer,[1] Thomas Walz,[2,3] and K. Christopher Garcia[1,4,*]
[1]Departments of Molecular and Cellular Physiology and Structural Biology, Stanford University School of Medicine, Stanford, CA 94305, USA
[2]Department of Cell Biology
[3]Howard Hughes Medical Institute
Harvard Medical School, 240 Longwood Avenue, Boston, MA 02115, USA
[4]Howard Hughes Medical Institute, Stanford University School of Medicine, Stanford, CA 94305, USA
[5]Present address: Life Sciences Institute & Department of Biological Chemistry, University of Michigan Medical School, Ann Arbor, MI, 48109, USA
[6]These authors contributed equally to this work
*Correspondence: kcgarcia@stanford.edu
DOI 10.1016/j.str.2010.10.010

SUMMARY

The shared cytokine receptor gp130 signals as a homodimer or heterodimer through activation of Janus kinases (Jaks) associated with the receptor intracellular domains. Here, we reconstitute, in parts and whole, the full-length gp130 homodimer in complex with the cytokine interleukin-6 (IL-6), its alpha receptor (IL-6Rα) and Jak1, for electron microscopy imaging. We find that the full-length gp130 homodimer complex has intimate interactions between the trans- and juxtamembrane segments of the two receptors, appearing to form a continuous connection between the extra- and intracellular regions. 2D averages and 3D reconstructions of full-length Jak1 reveal a three lobed structure comprising FERM-SH2, pseudokinase, and kinase modules possessing extensive intersegmental flexibility that likely facilitates allosteric activation. Single-particle imaging of the gp130/IL-6/IL-6Rα/Jak1 holocomplex shows Jak1 associated with the membrane proximal intracellular regions of gp130, abutting the would-be inner leaflet of the cell membrane. Jak1 association with gp130 is enhanced by the presence of a membrane environment.

INTRODUCTION

Cytokine-induced homo- or heterodimerization of cell surface receptors is a ubiquitous signaling paradigm in higher eukaryotes (Stroud and Wells, 2004; Wang et al., 2009). Cytokines of the four helix bundle family are required for the growth and differentiation of nearly all cell types, but are particularly important for regulation of the immune and hematopoietic systems. Activation of signaling involves homo- or heterodimerization of two receptors by a single cytokine molecule, as first illustrated by Human Growth Hormone (HGH) in complex with its receptor (HGH-R) (de Vos et al., 1992). This dimerization event initiates activation of Janus kinases (Jaks) that are bound to the intracellular domains of the receptors (Ihle, 1995). The active kinases then phosphorylate the C-terminal intracellular tails of the receptors on specific tyrosine residues, creating binding sites for pathway-associated signaling molecules such as STAT (signal transducer and activator of transcription) transcription factors which, upon phosphorylation by the active Jaks, translocate to the nucleus where they activate transcription of cytokine-responsive genes (Leonard and O'Shea, 1998).

Gp130 serves as a shared signaling receptor for at least eight different cytokines, including IL-6, IL-11, IL-27, Leukemia Inhibitory Factor (LIF), Oncostatin-M (OSM), Ciliary Neurotrophic Factor (CNTF), Cardiotrophin-1 (CT-1), and Cardiotrophin-like-cytokine (CLC) (Bravo and Heath, 2000; Wang et al., 2009). Gp130 has evolved a remarkable set of structural characteristics to facilitate shared signaling. First, gp130 has evolved cross-reactive cytokine binding sites that are structurally ideal for engaging a highly varied set of cytokines either alone (LIF, OSM) or with associated alpha receptor subunits (IL-6, IL-11, CNTF, CT-1, CLC) (Boulanger et al., 2003a; Boulanger and Garcia, 2004). Second, gp130 can homodimerize or heterodimerize with a second gp130 family receptor (LIFR, OSMR, TCCR) depending on the cytokine encountered (Heinrich et al., 2003).

Homodimerization of gp130, which occurs in response to the cytokines IL-6 and IL-11, occurs in a three step fashion, with the cytokine first binding to the ligand-specific alpha receptor (site 1), followed by binding to gp130 to form the signaling-competent hexamer (Boulanger et al., 2003b; Chow et al., 2001) that comprises the membrane-distal "headpiece" and membrane-proximal "legs" (Figure 1A). An electron microscopy (EM) study of the complete extracellular domains of gp130 bound to IL6/IL6-Rα indicated a convergence of the membrane proximal D6 "leg" domains of gp130 (Skiniotis et al., 2005). This finding was supported by a cryoelectron microscopic study of the IL-11/IL-11Rα/gp130 complex, where the legs also appeared to converge in a ring-like shape (Matadeen et al., 2007). A subsequent EM study on the full-length gp130/LIF-R/CNTF

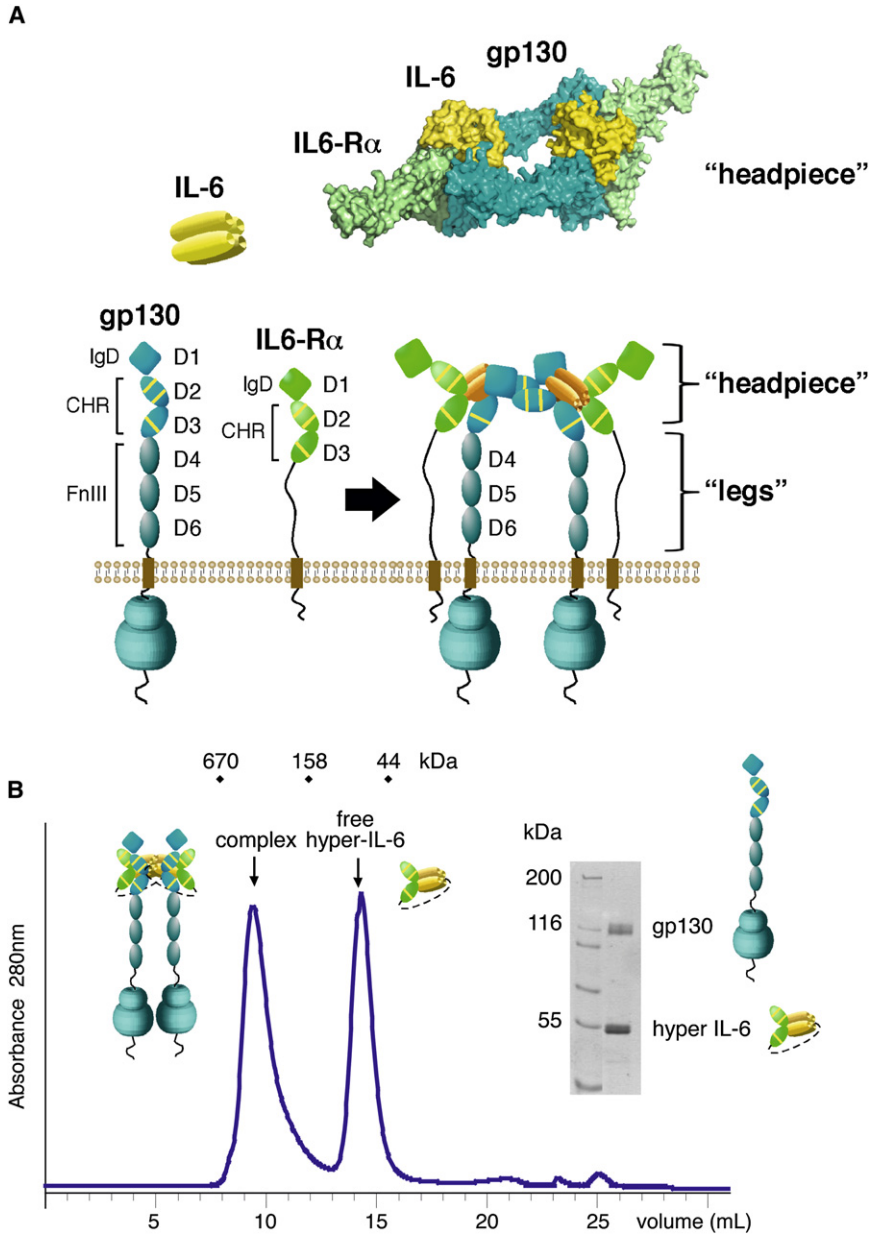

Figure 1. Assembly and Purification of the Full-Length gp130/IL-6/IL-6Rα Complex

(A) Components of the gp130/IL-6/IL-6Rα complex in pre- and postassembly state. A surface rendering of the structure of the signaling hexamer is shown on top. IgD denotes Ig-like domain, CHR denotes cytokine-binding homology region, and FnIII denotes Fibronectin-type III domain.

(B) Purification of the gp130/ IL6/IL6Rα complex by size exclusion chromatography.

complex, containing the TM segments and intracellular domains (ICDs), revealed a surprisingly intimate interaction between the extracellular juxtamembrane domains of gp130 and LIF-R (Skiniotis et al., 2008). Finally, a recent crystal structure of a complete, but unliganded, gp130 extracellular domain showed that, consistent with the EM studies, the gp130 legs are kinked at the D4-D5 boundary, and as a result would bend inward toward one another within the dimeric complex (Xu et al., 2010).

A critical piece of the puzzle to understand cytokine receptor signaling involves the Jak/Tyk family of intracellular kinases, which have remained enigmatic structurally (Leonard and O'Shea, 1998; Schindler et al., 2007). The Jak/Tyk family consists of four members, Jak1, Jak2, Jak3, and Tyk2, that are associated with cytokine receptors through a small membrane-proximal region of the ICD called the "Box 1/Box 2" (Haan et al., 2006; Murakami et al., 1991). The Jaks are ~1200 amino acid proteins that are subdivided by sequence into seven Janus homology regions (JH1-7) which fold into four distinct domains (Haan et al., 2006). The N terminus consists of a FERM domain, which mediates the interaction with cytokine receptors, followed by an SH2-like domain and a pseudokinase domain that lacks catalytic activity, and finally the C terminus is the active tyrosine kinase domain (KD). Several publications have suggested that Jak activation is regulated through interdomain communication, such as between the FERM and KD, requiring conformational change during signaling (Zhou et al., 2001). Further, disease-related mutations in Jaks have been speculated to interfere with the ability of Jak to undergo normal allosteric regulation (Funakoshi-Tago et al., 2008; Zhou et al., 2001). However, although several isolated KD structures have been reported (Boggon et al., 2005; Chrencik et al., 2010; Lucet et al., 2006), little is known about the structure of intact Jak family members.

In this study, we capitalize on the characteristic shape of the "tall" gp130 extracellular regions to visualize the full-length receptor holocomplex by single particle EM. We reconstitute and image a receptor signaling complex including IL-6, IL-6Rα, gp130, and Jak1, both in isolation, and in complex with each other. The EM images indicate that the full-length gp130/IL-6/IL-6Rα ternary complex forms a well-defined, structurally stabilized assembly with the juxtamembrane and transmembrane domains in intimate contact upon ligand binding. Projection averages and reconstructions of Jak1 show it to be a three-lobed molecule with conformational flexibility that could, in principle, facilitate interdomain communication. The holocomplex images suggest that homodimerization of gp130 by IL-6 locks the extracellular/transmembrane domains of gp130 together into continuous unit that can sensitively transduce a conformational signal through the plasma membrane to Jaks that are bound at the extreme juxtamembrane

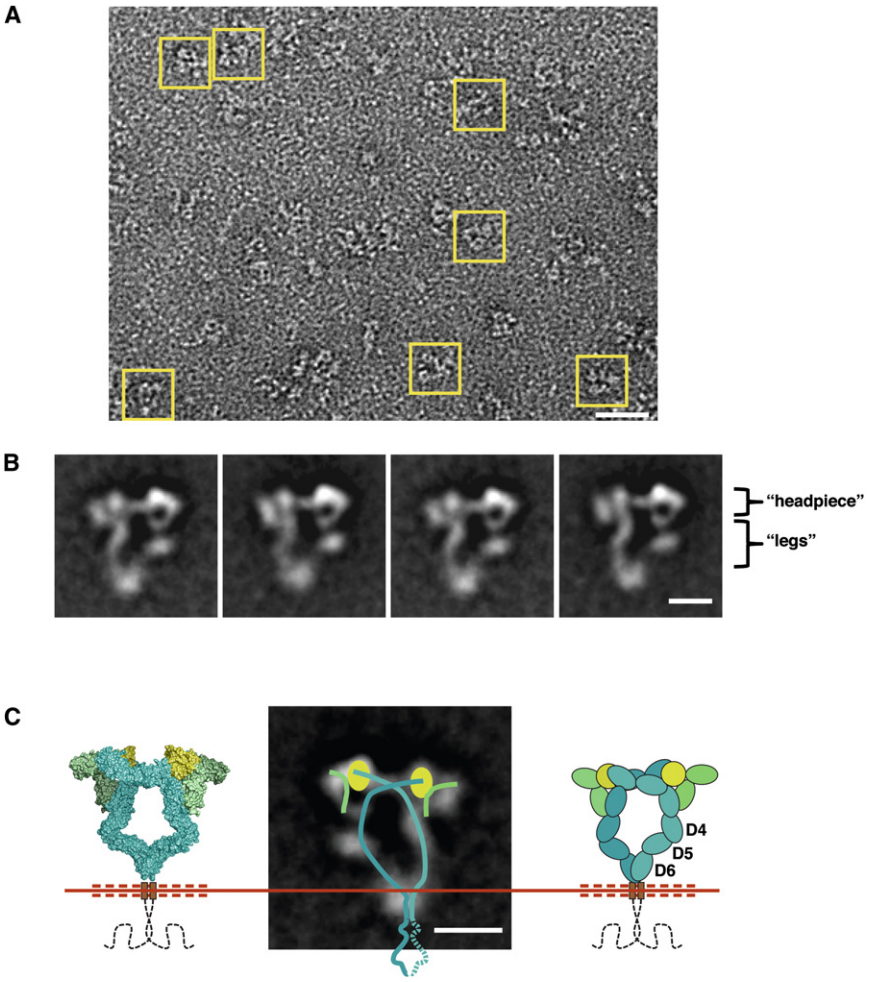

Figure 2. 2D EM Averages of the Full-Length gp130/IL-6/IL-6Rα Complex

(A) Raw image of negatively stained full-length gp130/IL-6/IL-6Rα complexes. Representative particles are boxed in yellow.

(B) 2D class averages of the gp130/hyper IL-6 complex produced by the classification of 6070 particles.

(C) Comparison of a 2D class average to a model based on the gp130/IL-6Rα/IL-6 complex (left). The cartoon on the right shows the domain organization of the gp130/ IL-6Rα/IL-6 complex. Lines overlaid on the 2D average trace the chains of the receptors and denote the location of the IL-6 cytokine.

Scale bars in (A) and (B) and (C) correspond to 40 and 10 nm, respectively.

See also Figure S1.

regions of the intracellular domains, likely interacting with the inner leaflet of the cell membrane.

RESULTS

Imaging the gp130/IL-6/IL-6Rα Transmembrane Complex

We took advantage of the highly characteristic and extended structure of gp130, which as a "tall" receptor has six extracellular domains, compared with two or three for most cytokine receptors, to attempt EM imaging of the full-length receptor (Figure 1A). The extracellular complex structure is a roughly triangular assembly containing the membrane-distal ligand binding "headpiece" and membrane-proximal "legs," and these obvious features serve as clear fiducial landmarks for particle identification on EM grids. As a prerequisite to reconstituting a complete IL-6/IL-6Rα/gp130/Jak1 quaternary signaling complex, we first purified and characterized the full-length ternary complex between IL-6, IL-6Rα, and gp130 in order to produce comparison images of the receptor complex with and without Jak1 included.

We expressed full-length gp130 in insect cells, with a C-terminal antibody epitope tag (EYMPME) and solubilized the receptor in the detergent n-dodecyl-β,D-maltoside (DDM). Gp130 was then captured from the detergent solubilized membranes by a Glu-Glu antibody affinity column and competitively eluted with soluble peptide. The eluate was then incubated with an excess of soluble IL-6/IL-6Rα fusion protein (also termed "hyper-IL6"; Fischer et al., 1997) to form the dimerized ternary complex (i.e., the hexamer), and further purified by size exclusion chromatography (Figure 1B). The complex was very stable and eluted from the column as a single peak of ~400 kDa, which is the approximate size of two receptors (2 × 110 kDa) and two hyper-IL-6 molecules (2 × 55 kDa), allowing ~90 kDa for the detergent micelle.

We then employed EM to visualize the complexes embedded in negative stain, which revealed monodisperse particles of similar size and shape (Figure 2A). Classification of 6070 particles (from 56 images taken on film) into 15 classes produced class averages that showed a dominant preferred particle orientation on the carbon support (see Figure S1 available online). As we have previously observed in the case of the extracellular gp130 complex (Skiniotis et al., 2005), the class averages of the full-length gp130 complex reveal a characteristic pseudo-two-fold symmetric particle, in which the gp130 leg domains (D4-D6) project from the cytokine binding headpiece containing IL-6 and IL-6Rα, and subsequently bend toward each other before joining at the their C-terminal tips at the level of the TM segments (Figures 2B and 2C). Strikingly, in contrast to the leg flexibility observed in the complex that contained only the extracellular domains of gp130 (Skiniotis et al., 2005), the class averages of the full-length gp130 complex containing TM segments indicate a conformationally rigid particle with uniform closure of the gp130 membrane-proximal domains (Figure 5, compare top and middle panels). The 2D averages here show homogenous leg positioning, with the D6 and transmembrane domains

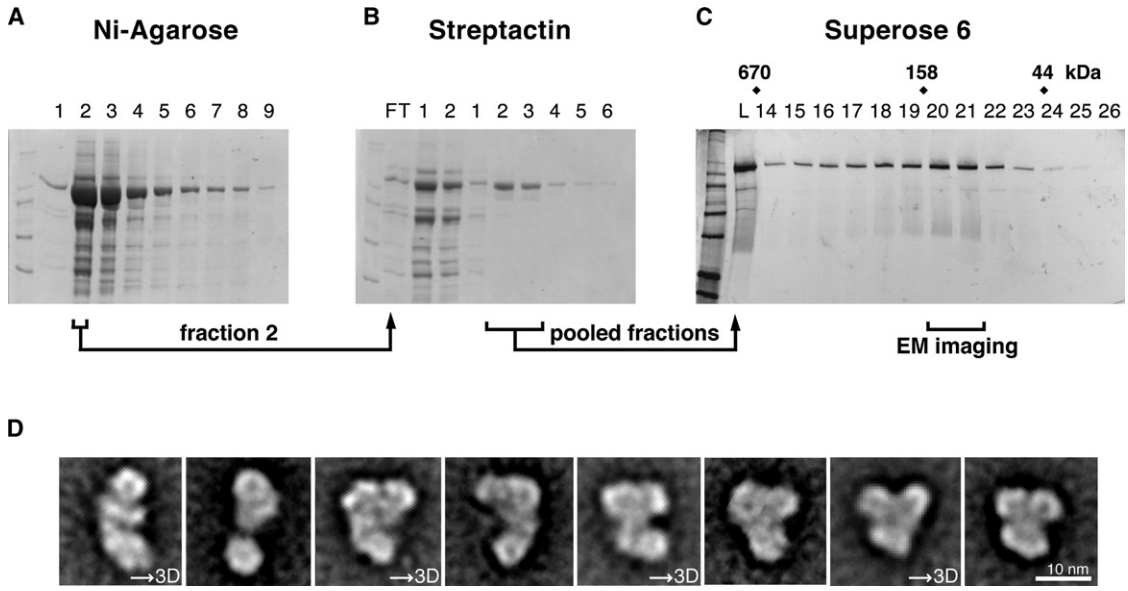

Figure 3. Purification and 2D Projections of Recombinant Human Jak1

(A) Jak1 was expressed using the BacMam system, and purified from 293S cell lysate via a C-terminal 8-Histidine tag using Ni-affinity column.

(B) Second step, streptactin-affinity purification of Jak1 via its N-terminal Strep-tag.

(C) Silver-stained gel of Streptactin-purified Jak1 after a Superose 6 size exclusion chromatography step. These fractions were selected for negative stain EM. See Figure S2.

(D) Representative 2D class averages of purified Jak1 obtained from the classification of 9258 particles. The marked classes were used independently for 3D reconstructions.

See also Figures S3–S5.

closely apposed. The presence of the TM segments in the complex may possibly stabilize the leg closure of gp130, as cytokine receptor TM helices have been proposed to self-associate within the membrane (Constantinescu et al., 2001; Kubatzky et al., 2001). Below the TM regions, little density was visible, indicating the intracellular domains of the gp130 homodimeric complex are loosely structured as seen in the gp130/LIFR heterodimeric complex (Skiniotis et al., 2008).

Purification and Imaging of Jak1

To generate sufficient quantities of Jak1 for imaging studies, we used the BacMam system and 293S cells (Figure 3; Dukkipati et al., 2008). Prior efforts to produce a variety of different full-length Jak molecules in insect cells resulted in aggregated and inactive material. The material from 293S cells is soluble, although it is not amenable to high protein concentrations, and solubility is enhanced by the presence of detergent (0.01% DDM). We utilized a three step purification scheme to purify Jak1 to >98% purity (Figures 3A–3C). Jak1 was first purified via a C-terminal 8-Histidine tag from 4 liters of 293S cell lysate using Nickel-agarose (Figure 3A), followed by Streptactin purification via an N-terminal Strep-tag (Figure 3B). The protein was then purified by size exclusion chromatography on Superose 6 to generate monodisperse Jak1 for EM imaging (Figure 3C). While the gel filtration elution peak was broad, a significant fraction of the material eluted at a position expected for monomeric Jak1. Additionally, the recombinant Jak1 we purified from mammalian cells was active at phosporylating the gp130 intracellular domain in kinase assays (Figure S2).

We again employed negative stain EM to visualize our preparations of Jak1 (Figure 3D). Raw images of Jak1 indicated a monodisperse particle population, albeit with a high degree of conformational variability (Figure S3). To analyze these conformers we interactively selected 24,356 particle pairs and used image classification to select the most consistent 9258 particles (Figure S4; see Experimental Procedures). After classification of the 9258 particles from the images of the untilted specimens into 50 classes (Figure S5), the resulting 2D class averages of Jak1 (representative 2D averages shown in Figure 3D) confirmed our suspicion of a highly flexible particle ranging from an extended to a compact conformation. In the class averages we can discern three main lobe densities, two in constant close proximity, and a third more globular, larger one in variable positions.

3D Reconstruction of Jak1

To gain further insight to the conformations presented by Jak1, and considering the high level of conformational variability observed, we used the corresponding particles selected from images of the tilted specimens to calculate separate 3D reconstructions for individual classes (containing from 446 to 1050 particles) produced by 2D classification (Figure 3D; Figure S5). While there are many classes evident, we focused our approach on three well-defined classes that exemplify intermediates in a transition from a fully extended to a compact conformation, as shown in Figure 4 (top panel-open to bottom panel-closed). 3D reconstructions were initially calculated by back-projection according to the random conical tilt method (Radermacher

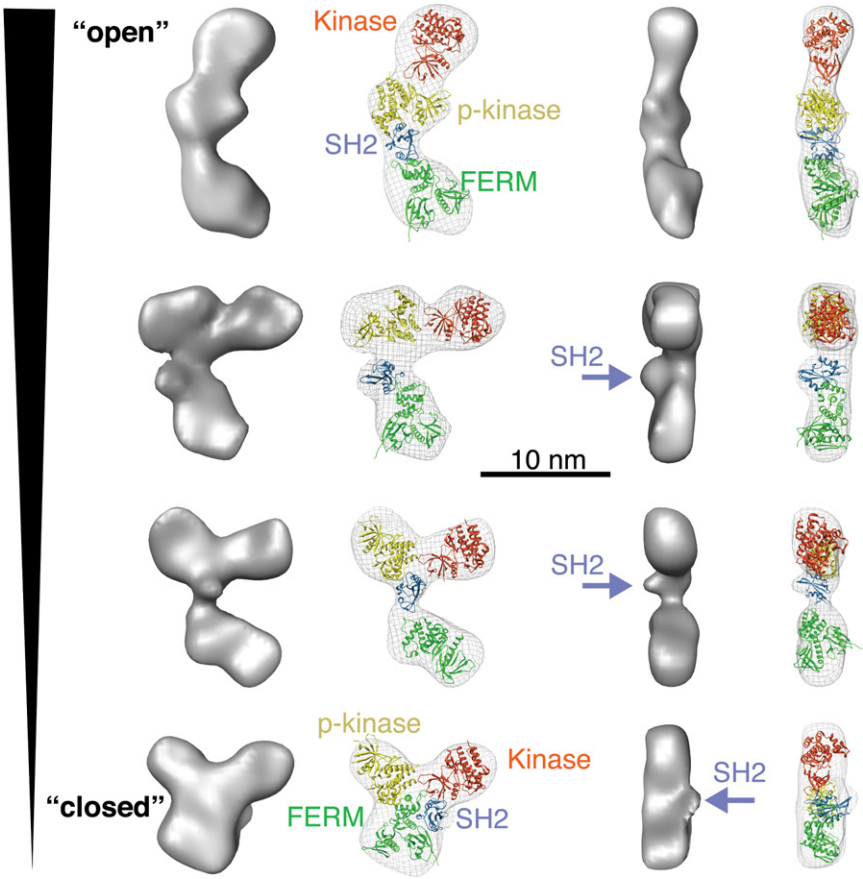

Figure 4. 3D Reconstructions and Modeling of Full-Length Human Jak1

3D reconstructions of Jak1 are based on individual classes obtained from 2D classification of untilted specimen projections (marked in Figure 3D and Figure S6). From the top to the bottom of the panel Jak1 particles transition from open to closed conformations. The FERM (green), SH2-like (cyan), pseudokinase (yellow), and kinase (red) domains of Jak1 were modeled into the EM densities. The orientations of the reconstructions in the left column of the panel are viewing the particles "face-on" the grid (as shown in the 2D class averages of Figure 3D), while the orientations to the right are rotated 90°, reflecting the flatness of the surface on which Jak1 is lying.
See also Figures S5 and S6.

et al., 1987) and further refined after the inclusion of 0° particle projections. The resulting 3D models at a resolution of ~35 Å (as judged by Fourier shell correlation) (Figure S6) reveal a highly asymmetric molecule displaying three major lobes (Figure 4). As also indicated in the 2D class averages (Figure 3D), two of the major lobes are always in close proximity, in what appear to be extended "longitudinal" interactions. In contrast, the third lobe appears as an individually larger, more globular domain that is loosely connected to the first two modules, thereby adopting variable positions with respect to the other two lobes. Interestingly, with the exception of the fully extended conformation ("open"), all reconstructions display an additional minor lobe, or "bump," which projects between the globular mobile and the two stable lobes, that is most likely the SH2 domain (indicated by arrows in Figure 4).

In order to interpret the densities revealed in our reconstructions we manually fit models of appropriate domains from available crystal structures into the density maps. To model the kinase and pseudokinase domains, we used two copies of the atomic resolution structure of the Jak1 kinase domain (PDB ID: 3EYH) (Chrencik et al., 2010). We used homologous crystal structures for the Focal Adhesion Kinase FERM domain (PDB ID: 2AL6) (Ceccarelli et al., 2006) and the Src SH2 domain (PDB ID: 1IJR) (Kawahata et al., 2001). Sequence comparisons indicate that the interdomain linker connecting the FERM-SH2 module with the pseudokinase module is approximately 20 amino acids long. Thus we reasoned that the larger globular lobe, loosely connected at one end of the EM density should correspond to the FERM domain, which appears to fit well in that position (Figure 4). In a next step, we modeled the SH2 domain at the border region between the FERM domain and two stable major lobes, thereby occupying the minor lobe shown in our 3D reconstructions. Subsequently, we docked the pseudokinase domain within the middle major lobe, which is immediately adjacent to the FERM-SH2 module, followed by the C-terminal kinase domain (KD). The 3D maps lack sufficient resolution to propose specific interactions between the individual domains of Jak1. However, our density maps and modeling argue that the FERM-SH2 module adopts variable conformations in relation to the pseudokinase-kinase module, and this is consistent with sequence analysis that indicates a longer linker between the FERM-SH2 and pseudokinase domains. In the compact Jak1 conformation, the close proximity of the FERM-SH2 module to the catalytic KD supports the possibility of a direct interaction as has been suggested by earlier biochemical studies (Funakoshi-Tago et al., 2008; Zhou et al., 2001), and analogous to that seen for Focal Adhesion Kinase (discussed later) (Lietha et al., 2007).

Preparation and Imaging of the gp130/IL-6/IL-6Rα/Jak1 Complex

To prepare the quaternary gp130/IL-6/IL-6Rα/Jak1 complex, purifications of the ternary gp130/IL-6/IL-6Rα complex and Jak1 were carried out concurrently. The gp130 complex was mixed with Jak1 purified from Streptactin, incubated overnight, and further purified by either anion exchange (Mono-Q) (Figure 5A) or size exclusion chromatography. Jak1 alone does not adhere strongly to mono-Q, but co-elutes as a complex with the receptor, although there is some dissociation during purification since the interaction does not appear to be high affinity. Raw EM images of our gp130/IL-6/IL-6Rα/Jak1 complex preparations in negative stain showed a significant fraction of bulkier

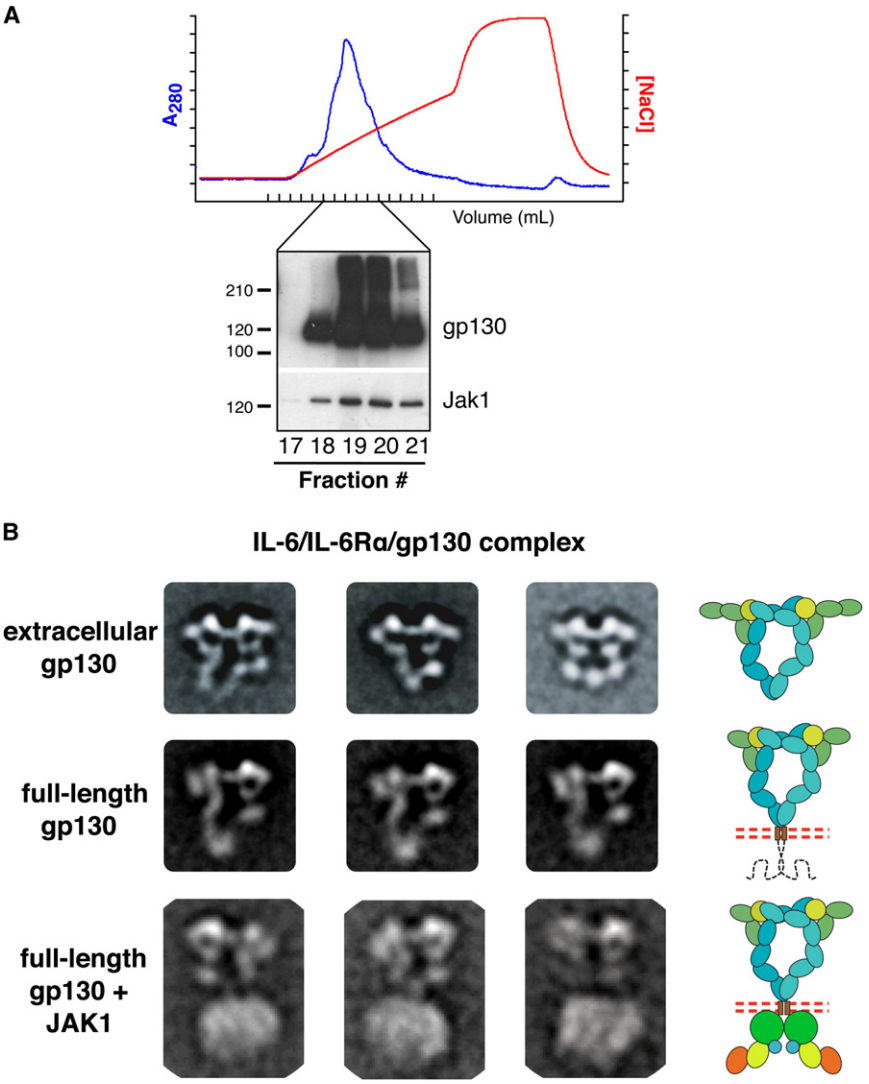

Figure 5. Purification and EM Imaging of the gp130/IL-6/IL-6Rα/Jak1 Complex

(A) Anion-exchange chromatography of the gp130/Jak1 complex. Fractions from the Mono-Q column were analyzed by SDS-PAGE gel and western blot with anti-GluGlu (gp130) and anti-Jak1 antibodies (panel underneath). Since two different antibodies were used to detect gp130 (Anti-GluGlu) and Jak1 (Anti-Jak1) the relative ratios of gp130/Jak1 cannot be derived from this experiment. The anti-GluGlu mAb appears to be more sensitive than anti-Jak1.

(B) Comparison of representative 2D averages for the soluble gp130/IL-6/IL-6Rα extracellular complex (top three panels), full-length gp130/IL-6/IL-6Rα (middle panels, as shown in Figure 2B), and the gp130/IL-6/IL-6Rα/Jak1 complex (bottom three panels). Schematics for each complex are shown in the far right column. The extra fuzzy density in the Jak1 loaded complexes is apparent by comparison to the non-loaded complexes. See also Figures S7 and S8.

particles when compared to full-length receptor in the absence of Jak1 (Figure S7). We were able to easily discern the characteristic side views of the extracellular domains and headpiece, as seen in the soluble and full-length receptor complex EM images not containing Jak1, with significant additional mass following the membrane proximal FNIII legs and TM regions (Figure 5B, bottom row). We selected 14,008 particles from 224 images taken on imaging plates, of which 3975 particles (see Materials and Methods) were used for the final classification into 30 classes (Figure S8). Most of the resulting class averages show the clear pseudo-two-fold symmetric densities representing the extracellular regions of the receptor complex (representative class averages shown in Figure 5B, bottom panels). Directly below the transmembrane level we observe additional density that can only represent the bound Jak1. In fact, direct comparison of the "unloaded" gp130/IL-6/IL-6Rα ternary complex to that "loaded" with Jak1 clearly shows its position (compare Figure 5B middle and bottom rows). However, the Jak1 densities appear "fuzzy" and are not well resolved. This is likely due to variability in the Jak1 molecule conformations, and also variable orientations of Jak1 on the carbon support. This conformational mixture is probably also amplified by the flexible nature of the gp130 intracellular domains to which Jak1 is bound. Nevertheless, Jak1 appears to bind near the base of the TM region, at the extreme membrane proximal region of the gp130 ICD, where its binding site has been mapped (Haan et al., 2002).

Given the apparent "free swinging" of the Jak1/ICD module underneath the TM segment in the detergent-solubilized receptor complex, and the proximity of the inner leaflet of the membrane bilayer in the cell, we were curious if the addition of a bilayer environment might stabilize the Jak1 interaction. Therefore we reconstituted gp130/IL-6/IL-6Rα complexes in nanodiscs, which provide a bilayer surrounding the TM region (Figure 6). The nanodisc reconstitution was highly efficient for the gp130 complex using the MSP-1 protein and lipid to displace the detergent micelle. We were able to purify the ternary complex by gel filtration in the absence of detergent. We then added purified recombinant Jak1 to the gp130/IL-6/IL-6Rα nanodisc, and subjected the mixture to gel filtration (Figure 6). We found that the association of Jak1 with gp130 was far more stable and efficient than in detergent micelles (Figure 5), and the resultant holocomplex could be purified in nearly a stoichiometric ratio, with little Jak1 dissociation.

DISCUSSION

Our mechanistic understanding of communication between cytokine recognition and intracellular Jak/Tyk activation is poor compared to systems such as receptor Tyrosine Kinase's

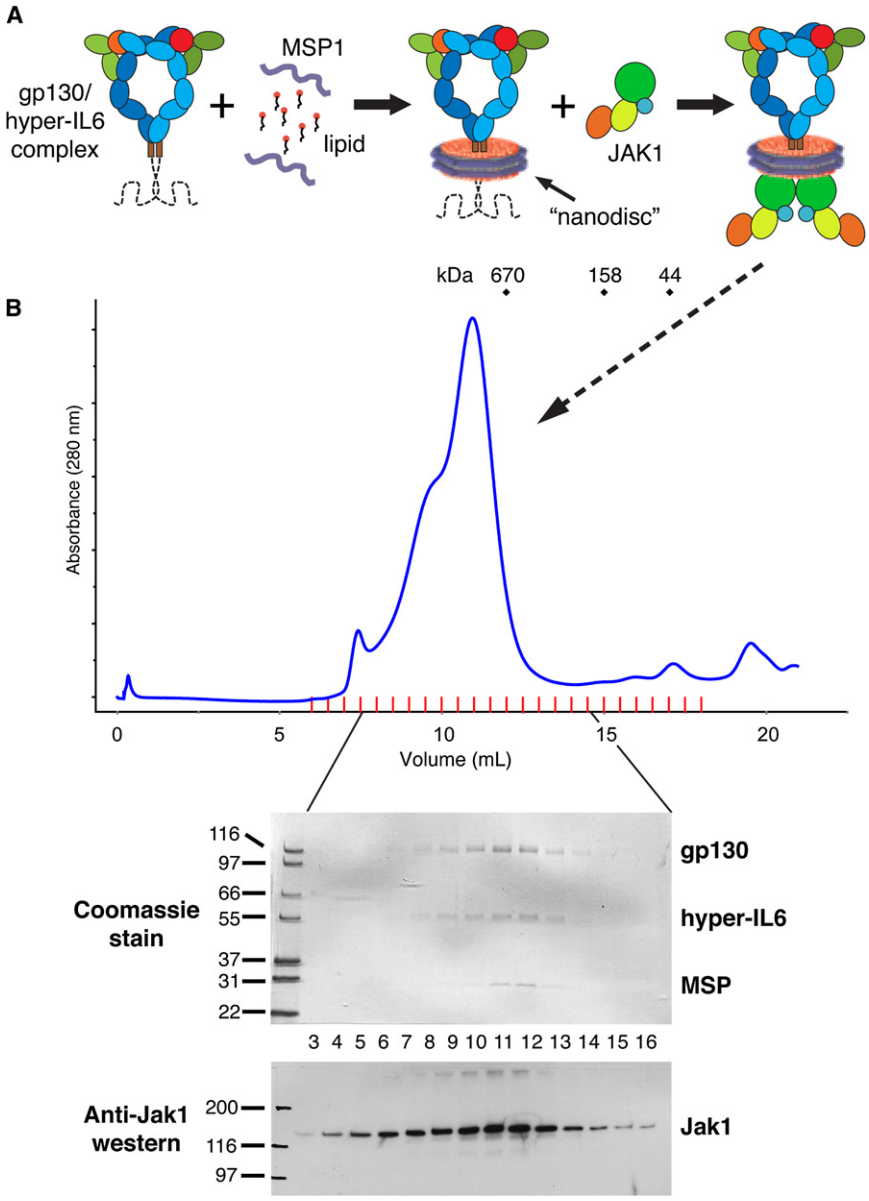

Figure 6. Reconstitution of the gp130/IL-6/IL-6Rα/Jak1 Complex in Lipid Nanodiscs

(A) The quaternary gp130/IL-6/IL-6Rα/Jak1 complex was prepared and incorporated into lipid "nanodiscs" comprising DPPC and the MSP1 scaffold protein, and purified by gel filtration chromatography (Superose 6) in the absence of detergent.

(B) Jak1 was then added to the nanodiscs containing gp130/ gp130/IL-6/IL-6Rα and again applied to a Superose 6 size exclusion column. Since full-length Jak1 and gp130 comigrate on SDS-PAGE, peak fractions were subjected to SDS-PAGE and Coomassie staining (top panel) and western blotting with an anti-Jak1 antibody (bottom panel) in order to confirm the presence of both components. Higher resolution SDS-PAGE and Coomassie confirms that both proteins are present in roughly equal amounts.

(RTK's), and Death receptors. The principal challenges to making progress on this problem have been the historic recalcitrance of Jak expression, and the difficulties posed by intact single-pass TM receptors for structural studies. Our strategy was to produce full-length Jak1 for EM analysis both alone and in complex with full-length gp130, and this has enabled us to report the first structural snapshots of Jak1, as well as of a fully "loaded" transmembrane receptor complex. While the mechanistic insight that can be gained from our studies is limited, the results we show here are informative on several levels. Our choice of gp130 was driven by its very characteristic extracellular structure by single-particle EM, which allows us to rapidly identify and orient particles. These studies demonstrate imaging of the cytokine receptor holocomplex is technically feasible, and that higher resolution imaging methodologies combined with nanodisc stabilization could lead to deeper mechanistic insights.

Imaging of the gp130/IL-6/IL-6Rα Complex

Two previous single-particle EM studies of gp130 complexes with IL-6 and IL-11, respectively, included only the extracellular domains of gp130 (Matadeen et al., 2007; Skiniotis et al., 2005). In the gp130/IL-6/IL-6Rα study, the majority of particles showed the gp130 leg domains together at the level of the membrane, but a number of other "open" conformations were observed, indicating that the leg domains were not necessarily holding the transmembrane domains together. In the IL-11/IL-11Rα/gp130 ectodomain complex, normal-mode analysis of the ring-like structure indicated a high degree of conformational flexibility in the leg regions that was speculated to facilitate rearrangement during signaling. In the current study, we observe that when the transmembrane and intracellular domains are included, the gp130 leg domains uniformly converge at the level of the membrane, and form an apparently continuous, possibly rigidified unit together with the transmembrane segments. This interaction is consistent with functional data suggesting critical interactions between the membrane proximal domains of gp130, where antagonistic antibodies map to the D4-D6 region of gp130 (Kurth et al., 2000). Association of the TM regions is also in accord with studies on EPO and Prolactin receptors showing the TM helix packing interactions within cytokine receptor dimers may be prevalent (Constantinescu et al., 2001; Kubatzky et al., 2001). Our prior EM imaging studies of the heterocomplex of full-length gp130 and LIF-R in complex with CNTF/CNTF-Rα, also indicated that the leg and TM domains were intimately associated upon ligand binding (Skiniotis et al., 2008).

The gp130 leg domains are "kinked" near the D4-D5-D6 boundaries, forcing the trajectory of the legs toward the center of the complex, enabling the juxtamembrane and transmembrane domains to be in close proximity. Indeed, a kink is also observed in this region of the D5 domain of gp130 in the gp130/LIFR/CNTF/CNTF-Rα complex (Skiniotis et al., 2008), and an acute bend between the D4 and D5 domains is observed in the crystal structure of the entire gp130 extracellular domain (Xu et al., 2010). Thus, the compendium of gp130 structures, both crystallographic and EM, suggest that the gp130 legs are bent, and in intimate association within the active signaling complex. Although we cannot visualize the TM interactions in detail at the resolution of the EM analysis, the structural evidence suggests that the close association of the membrane proximal regions of the legs is most likely assisted by packing interactions between the TM helices within the dimer, forming a continuous unit between the extracellular juxtamembrane regions and the TM. Thus, this possible packing between the TM helices of cytokine receptor dimers may be a general means of rigidifying the linkage between extracellular cytokine recognition and intracellular signaling. Such a rod-like unit would facilitate the transmission of subtle receptor positional differences to the intracellular signaling components by propagating, rather than absorbing extracellular torque. A similar model has been previously proposed based on structure-function studies of the EPO receptor (Seubert et al., 2003).

Imaging of Jak1

Our current structural knowledge of the Jak/Tyk family is limited to the obvious homologies of individual domains to known folds, such as the FERM, SH2 and pseudokinase domains, and crystal structures of several Jak KD's, including Jak1. But it is important to structurally characterize a full-length Jak given the apparent interdomain communication required for activation. 2D class averages and 3D reconstructions of full-length Jak1 indicate that the four major subdomains fold into three modules: (1) the larger FERM module, (2) an extended pseudo-kinase and kinase module, and (3) a module consisting of a smaller domain between the lobes that is likely the SH2-like domain (Figure 4). It is clear from our analysis that the Jak1 subdomains are highly flexible with respect to one another, and can exist in wide array conformations ranging from open to closed. Our results also suggest that the kinase and pseudokinase subdomains are closely associated with one another, forming a rather continuous bi-lobed module. This configuration differs from the JH1-JH2 domain relationship predicted from a homology modeling study of Jak2 that was based on the FGF receptor kinase dimer structure (Lindauer et al., 2001). Several previous studies have suggested that regulation of the C-terminal KD takes place through its interactions with the N-terminal FERM domain, which would necessitate a compact state of Jak (Saharinen and Silvennoinen, 2002; Zhou et al., 2001). Coexpression of the isolated FERM domain with the isolated KD of Jak1, and deletion of the pseudokinase domain in Jak2 and Jak3, enhances KD activity. These findings suggest that: (1) the "active" form of Jak requires close proximity between the N- and C-terminal domains, and (2) a role of the pseudokinase domain may be to sterically interfere with Jak KD activation until receptor dimerization initiates a conformational change in Jak. Interestingly, in the compact Jak1 conformation we see by EM, the FERM and SH2 domains come in very close proximity to the catalytically active C-terminal KD, consistent with the biochemical studies (Zhou et al., 2001). Therefore, the built-in flexibility of Jak1 may facilitate regulation of KD activity by allowing Jak1 to shuttle between open and closed states. It was speculated recently that cytosolic Jak2 may be "locked" into an inactive compact state until its FERM domain engages the receptor (Funakoshi-Tago et al., 2008). Contrary to this model, our "free-floating" Jak1 reveals a highly diverse conformational ensemble relatively evenly dispersed between open and closed states, and partial open/closed states, that does not appear to be locked into a particular structure. However, we cannot say whether, or if, the open or closed conformations correspond to active or inactive Jak1. In order to address this, we have attempted to lock Jak1 into a compact state using linkers and other engineering approaches, but have so far been unsuccessful.

Focal Adhesion Kinase (FAK) has structural analogies to Jak/Tyk kinases, since FAK possesses an N-terminal FERM domain and a C-terminal KD. In the structure of autoinhibited FAK, the FERM and KD are in direct contact such that the FERM prevents access to the KD phosphorylation sites, whereas in the activated state, the FERM interaction is relieved (Lietha et al., 2007). Like FAK, Jak1 also possesses an N-terminal FERM and C-terminal KD that we see by EM exist in highly variable positions relative to one another, either in contact in the compact conformation, or far apart in the open conformation. The analogy to FAK suggests that the compact Jak1 conformation may represent an "inactive" conformation, in which the KD is autoinhibited by FERM interactions. However, unlike FAK, in Jak1 the FERM/KD interaction does not appear to be stable in solution in that the particles do not preferentially segregate into a close state. There is also the further consideration that FAK is a freely diffusing molecule within the cytosol, whereas Jak/Tyk proteins are primarily associated with cytokine receptors, which almost certainly influence Jak conformation. Thus, the receptor-bound form is, indeed, a more physiologically relevant state in which to image Jak, and this is where our efforts are directed.

The gp130/IL-6/IL-6Rα/Jak1 Complex

We prepared gp130/IL-6/IL-6Rα ternary complexes both in detergent micelles as well as in lipid "nanodiscs" that reconstitute a more physiological environment for transmembrane helices. Holocomplexes in detergent micelles were subjected to negative staining and EM imaging. The characteristic two-fold symmetric extracellular domains of gp130/IL-6/IL-6Rα are well resolved in the 2D averages. Below the TM region, a fuzzy density is observed that likely corresponds to bound Jak1 molecules, but the density cannot be fit with any Jak1 domains given its smeared character.

Imaging of the holocomplex denotes a proof-of-concept technical benchmark that requires substantial improvement before detailed structural conclusions can be reached. However several important facts have emerged from these experiments. First, our initial attempts to form complexes between Jak1 and an isolated soluble gp130 ICD were not successful, since the two components dissociated over gel filtration, indicating a very low affinity interaction (data not shown). Association of Jak1 with the full-length gp130 in detergent micelles was far

more efficient and lead to the isolation of complexes. Thus, the membrane/lipid environment appears to be important for Jak1 association with gp130 and by extension, perhaps, other cytokine receptors. Second, while Jak1 is present, it appears to exist as a conformational ensemble in the complex, as evidenced by the "fuzzy" density. We have previously shown that the gp130 intracellular domains are highly flexible, and not visible by 2D imaging (see Figure 2) (Skiniotis et al., 2008). The Box1/Box2 sequence region of gp130, to which the Jak1 FERM domain binds, is located at the extreme N-terminal region of the gp130 ICD (directly after the TM), and this is where we see the Jak1 density in the holocomplex. Presumably the uppermost part of the density corresponds to the FERM domains, while the density further away from the TM region of gp130 corresponds to the more C-terminal domains of Jak1 that are likely "free-swinging" since Jak1 is only bound to gp130 via its FERM. The nature of this single site Jak1-FERM/gp130 contact preserves the Jak1 interdomain flexibility that is likely necessary for the mechanism of Jak1 activation. The KD can, in principle, associate with the FERM, and then once activated, analogous to an unfolding scorpion's tail, phosphorylate STAT and other adaptors that are known to bind to the C-terminal regions of the gp130 ICD. Unfortunately, this flexibility prevents us from trapping the complex in a single position that will allow structural definitions to emerge. Therefore, these studies show that while it is indeed feasible to reconstitute the gp130 signaling holocomplex, future attempts will need to address the positional variability of the Jak/ICD module.

The holocomplex is greatly stabilized in nanodiscs, which provide a surrogate membrane bilayer. Our speculation is that the inner leaflet of the nanodisc is in contact with the Jak1 FERM domain that is bound to the Box1/Box2 near the membrane, stabilizing the interaction. The size of the FERM domain, coupled with the close proximity of the Box1/Box2 region to the TM segments of cytokine receptors, makes this a plausible scenario, especially considering the fact that our recombinant Jaks seem to require detergent for stability. Perhaps the FERM possesses a hydrophobic patch that is in contact with the membrane. Future attempts to visualize the gp130/Jak1 holocomplex will focus on cryoelectron microscopy of nanodisc-reconstituted complex.

EXPERIMENTAL PROCEDURES

Expression and Purification of the gp130/IL-6/IL-6Rα Complex

Full-length gp130 was expressed as previously described (Skiniotis et al., 2008). In brief, full-length, EYMPME-tagged gp130 was expressed in HiFive cells, cell membranes were isolated and solubilized in 1% n-dodecyl-β-d-maltoside (DDM), and recombinant receptors were purified via an anti-Glu-Glu-sepharose column. A soluble construct of human IL-6 fused to the D2-D3 cytokine binding region of IL-6Rα (hyper IL-6) (Fischer et al., 1997) was expressed and purified from HiFive cell supernatant via Ni-affinity and gel filtration chromatography. An excess of hyper-IL-6 was added to the purified gp130 and incubated overnight. The protein mixture was then concentrated and purified on a Superdex 200 column equilibrated in HEPES-buffered saline containing 100 μM DTT and 0.02% DDM.

Expression and Purification of Jak1

Full-length human Jak1 was cloned into the BacMam expression vector pVLAD6 (Dukkipati et al., 2008), and recombinant baculoviruses were prepared in SF9 insect cells. 293S cells were grown in suspension in Pro293 media (Lonza, Inc.), infected with Jak1 baculoviruses, and protein expressed for 24 hr at 37°C. Cells were pelleted, resuspended in buffer A (20 mM Tris-HCl [pH 8.0], 1 mM TCEP, and protease inhibitors) and dounce homogenized to lyse the cells. Insoluble material was pelleted at ~45,000 × g for 1 hr at 4°C, and the supernatant harvested. To the supernatant was added 500 mM NaCl, 0.1% DDM, 20 mM imidazole, and 5% glycerol, and the lysate was incubated with Ni-agarose affinity beads in batch for 2 hr. Beads were then collected and washed with buffer B (20 mM Tris-HCl [pH 8.0], 150 mM NaCl, 1 mM TCEP, 0.02% DDM, 5% glycerol) containing 20 mM imidazole, followed by elution of Jak1 from the beads in buffer B containing 200 mM imidazole. After nickel elution, Jak1 elutions were loaded onto a Streptactin-sepharose column, washed with buffer B, and eluted in buffer B containing 2.5 mM desthiobiotin. Following elution from the Streptactin column, NaCl and glycerol to 500 mM and 20% were added, respectively, in order to stabilize Jak1 in solution. Glycerol was dialyzed from the Jak1 fractions immediately prior to EM imaging. Detection of Jak1 was performed by Coomassie staining and by western blot with an anti-Jak1 antibody (BD Biosciences 610231). The kinase activity of purified Jak1 is described in Figure S2.

Electron Microscopy

Receptor complexes and Jak1 were prepared for electron microscopy using the conventional negative staining protocol (Ohi et al., 2004), and imaged at room temperature with a Tecnai T12 electron microscope operated at 120 kV using low-dose procedures. Images of the hyper-IL-6/gp130 complex were recorded on Kodak SO-163 film at a magnification of 52,000× and a defocus value of about −1.5 μm. Images of Jak1 and the hyper-IL-6/gp130/Jak1 complex were recorded on imaging plates (DITABIS, Digital Biomedical Imaging Systems AG) at a magnification of 67,000× and a defocus value of about −1.0 μm.

Image Processing

Film recorded micrographs were digitized with a Zeiss SCAI scanner using a step size of 7 mm, and 3 × 3 pixels were averaged to obtain a pixel size of 4.04 Å on the specimen level. Imaging plates were analyzed with a DITABIS micron plate reader, and 2 × 2 pixels were averaged to obtain a pixel size of 4.48 Å on the specimen level.

Multireference alignment and classification for the projection analysis of all samples was carried out using the SPIDER image processing suite (Frank et al., 1996).

For the 2D analysis of the gp130/IL-6/IL-6Rα transmembrane complex we interactively selected 6070 particles from 56 images taken on film. The particles were classified into 15 classes, producing consistent class averages that showed a dominant preferred particle orientation on the carbon support (Figure S1).

For 2D analysis and 3D reconstructions of Jak1 we interactively selected 24,356 particle pairs from 132 60°/0° image pairs taken on imaging plates. A first round of classification of the untilted specimen into 100 classes (Figure S4) revealed a substantial degree of conformational variability. As a result, several class averages were not well defined, either revealing particles of smaller size or particles that lacked distinct features. We thus selected the particles belonging to the better defined classes (marked with a green dot in Figure S4; total of 9258 particles), and subjected them to a second round of classification into 50 classes (Figure S5). Based on this second classification step, four independent 3D reconstructions were derived from 446 to 1050 particles belonging to single classes that revealed a range of JAK1 conformations, from fully extended ("open") to fully compact ("closed") (the classes used for 3D reconstruction are marked in Figure 3D and Figure S5). In brief, the random conical tilt technique (Radermacher et al., 1987) was used to calculate a first back projection map using the images of the tilted specimen. After angular refinement, the corresponding particles from the images of the untilted specimens were added and the images were subjected to another cycle of angular refinement. Using the resulting maps as reference models, we calculate final 3D reconstructions with the program FREALIGN (Stewart and Grigorieff, 2004). FREALIGN was also used for further refinement of the orientation parameters as well as for correction of the contrast transfer function (CTF). The resolution of the final density map was ~35 Å according to Fourier shell correlation (FSC) using the FSC = 0.5 criterion (Figure S6).

For the 2D analysis of the quarternary gp130/IL-6/IL-6Rα/Jak1 transmembrane complex we interactively selected 14,008 particles from 224 images taken on imaging plates (Figure S7). After a first classification into 150 groups, we selected 3975 particles from those classes that clearly resolved the receptor complex ectodomain, and subjected them to a final classification into 30 classes (Figure S8).

Molecular Modeling of Jak1

Docking, modeling, and molecular graphics for Jak1 were generated using the UCSF Chimera package from the Resource for Biocomputing, Visualization, and Informatics at the University of California, San Francisco (Pettersen et al., 2004). Due to the limited resolution of our maps (~35 Å) we only employed manual procedures to dock crystal structures into the 3D densities. To model the kinase and pseudokinase domains we used two copies of the atomic resolution structure of the Jak1 kinase domain (PDB ID: 3EYH) (Williams et al., 2009). The Jak1 FERM domain was modeled using the homologous Focal Adhesion Kinase FERM domain (PDB ID: 2AL6) (Ceccarelli et al., 2006), whereas the Jak1 SH2 domain was modeled using a Src tyrosine kinase SH2 domain (PDB ID: 1IJR) (Kawahata et al., 2001).

Preparation of gp130/IL-6/IL-6Rα Nanodiscs

Nanodiscs were prepared using standard procedures essentially as described (Ritchie et al., 2009). 1,2-Dipalmitoyl-sn-glycero-3-phosphocholine (DPPC, Avanti Polar Lipids), dried overnight in a centrifugal evaporator, was solubilized in 100 mM cholate (Na cholate hydrate, SIGMA) (end concentration of DPPC: 50 mM) and incubated with membrane scaffold protein MSP1 and gp130-hyper-IL-6 complex at 37°C for 15 min at end concentrations of 7 mM (DPPC), 18 mM (cholate), 78 μM (MSP1), and 5.6 μM (gp130-hyper-IL-6 complex), respectively. The mixture was supplemented with 0.02% (w/v) n-dodecyl-β-D-maltopyranoside, 0.2% (v/v) 2-mercaptoethanol, and 1 mM phenylmethylsulfonyl fluoride (PMSF), respectively. After the incubation period at 37°C, 475 mg wet Bio-Beads SM-2 (BIO-RAD), washed with methanol and water, were added to the sample and incubated at 4°C for 9 hr on a rotating wheel to remove the detergent and initiate nanodisc self-assembly. The sample was subsequently analyzed by gel filtration on a Superose 6 column in 10 mM HEPES (pH 7.2), 150 mM NaCl, and 0.2% (v/v) 2-mercaptoethanol. We observed highly efficient nanodisc formation, and the complex eluted on gel filtration as a monodisperse peak.

SUPPLEMENTAL INFORMATION

Supplemental Information includes eight figures and can be found with this article online at doi:10.1016/j.str.2010.10.010.

ACKNOWLEDGMENTS

We thank Stefan Rose-John for helpful discussion and gift of the hyper-IL6 cDNA. The molecular EM facility at Harvard Medical School was established with a generous donation from the Giovanni Armenise Harvard Center for Structural Biology (T.W.). P.J.L. and G.S are Damon Runyon Fellows, supported by the Damon Runyon Cancer Research Foundation (DRG-1928-06 to P.J.L. and DRG-1824-04 to G.S.). C.T. is supported by a postdoctoral fellowship of the International Human Frontier Science Program Organization. This work was funded, in part, by an NIH grant (AI51321) to K.C.G. K.C.G. and T.W. are Investigators of the Howard Hughes Medical Institute.

Received: August 9, 2010
Revised: September 25, 2010
Accepted: October 31, 2010
Published: January 11, 2011

REFERENCES

Boggon, T.J., Li, Y., Manley, P.W., and Eck, M.J. (2005). Crystal structure of the Jak3 kinase domain in complex with a staurosporine analog. Blood *106*, 996–1002.

Boulanger, M.J., and Garcia, K.C. (2004). Shared cytokine signaling receptors: structural insights from the gp130 system. Adv. Protein Chem. *68*, 107–146.

Boulanger, M.J., Bankovich, A.J., Kortemme, T., Baker, D., and Garcia, K.C. (2003a). Convergent mechanisms for recognition of divergent cytokines by the shared signaling receptor gp130. Mol. Cell *12*, 577–589.

Boulanger, M.J., Chow, D.C., Brevnova, E.E., and Garcia, K.C. (2003b). Hexameric structure and assembly of the interleukin-6/IL-6 alpha-receptor/gp130 complex. Science *300*, 2101–2104.

Bravo, J., and Heath, J.K. (2000). Receptor recognition by gp130 cytokines. EMBO J. *19*, 2399–2411.

Ceccarelli, D.F., Song, H.K., Poy, F., Schaller, M.D., and Eck, M.J. (2006). Crystal structure of the FERM domain of focal adhesion kinase. J. Biol. Chem. *281*, 252–259.

Chow, D., Ho, J., Nguyen Pham, T.L., Rose-John, S., and Garcia, K.C. (2001). In vitro reconstitution of recognition and activation complexes between interleukin-6 and gp130. Biochemistry *40*, 7593–7603.

Chrencik, J.E., Patny, A., Leung, I.K., Korniski, B., Emmons, T.L., Hall, T., Weinberg, R.A., Gormley, J.A., Williams, J.M., Day, J.E., et al. (2010). Structural and thermodynamic characterization of the TYK2 and JAK3 kinase domains in complex with CP-690550 and CMP-6. J. Mol. Biol. *400*, 413–433.

Constantinescu, S.N., Keren, T., Socolovsky, M., Nam, H., Henis, Y.I., and Lodish, H.F. (2001). Ligand-independent oligomerization of cell-surface erythropoietin receptor is mediated by the transmembrane domain. Proc. Natl. Acad. Sci. USA *98*, 4379–4384.

de Vos, A.M., Ultsch, M., and Kossiakoff, A.A. (1992). Human growth hormone and extracellular domain of its receptor: crystal structure of the complex. Science *255*, 306–312.

Dukkipati, A., Park, H.H., Waghray, D., Fischer, S., and Garcia, K.C. (2008). BacMam system for high-level expression of recombinant soluble and membrane glycoproteins for structural studies. Protein Expr. Purif. *62*, 160–170.

Fischer, M., Goldschmitt, J., Peschel, C., Brakenhoff, J.P., Kallen, K.J., Wollmer, A., Grotzinger, J., and Rose-John, S. (1997). I. A bioactive designer cytokine for human hematopoietic progenitor cell expansion. Nat. Biotechnol. *15*, 142–145.

Frank, J., Radermacher, M., Penczek, P., Zhu, J., Li, Y., Ladjadj, M., and Leith, A. (1996). SPIDER and WEB: processing and visualization of images in 3D electron microscopy and related fields. J. Struct. Biol. *116*, 190–199.

Funakoshi-Tago, M., Pelletier, S., Moritake, H., Parganas, E., and Ihle, J.N. (2008). Jak2 FERM domain interaction with the erythropoietin receptor regulates Jak2 kinase activity. Mol. Cell. Biol. *28*, 1792–1801.

Haan, C., Heinrich, P.C., and Behrmann, I. (2002). Structural requirements of the interleukin-6 signal transducer gp130 for its interaction with Janus kinase 1: the receptor is crucial for kinase activation. Biochem. J. *361*, 105–111.

Haan, C., Kreis, S., Margue, C., and Behrmann, I. (2006). Jaks and cytokine receptors—an intimate relationship. Biochem. Pharmacol. *72*, 1538–1546.

Heinrich, P.C., Behrmann, I., Haan, S., Hermanns, H.M., Muller-Newen, G., and Schaper, F. (2003). Principles of interleukin (IL)-6-type cytokine signalling and its regulation. Biochem. J. *374*, 1–20.

Ihle, J.N. (1995). Cytokine receptor signalling. Nature *377*, 591–594.

Kawahata, N., Yang, M.G., Luke, G.P., Shakespeare, W.C., Sundaramoorthi, R., Wang, Y., Johnson, D., Merry, T., Violette, S., Guan, W., et al. (2001). A novel phosphotyrosine mimetic 4′-carboxymethyloxy-3′-phosphonophenylalanine (Cpp): exploitation in the design of nonpeptide inhibitors of pp60(Src) SH2 domain. Bioorg. Med. Chem. Lett. *11*, 2319–2323.

Kubatzky, K.F., Ruan, W., Gurezka, R., Cohen, J., Ketteler, R., Watowich, S.S., Neumann, D., Langosch, D., and Klingmuller, U. (2001). Self assembly of the transmembrane domain promotes signal transduction through the erythropoietin receptor. Curr. Biol. *11*, 110–115.

Kurth, I., Horsten, U., Pflanz, S., Timmermann, A., Kuster, A., Dahmen, H., Tacken, I., Heinrich, P.C., and Muller-Newen, G. (2000). Importance of the membrane-proximal extracellular domains for activation of the signal transducer glycoprotein 130. J. Immunol. *164*, 273–282.

Leonard, W.J., and O'Shea, J.J. (1998). Jaks and STATs: biological implications. Annu. Rev. Immunol. *16*, 293–322.

Lietha, D., Cai, X., Ceccarelli, D.F., Li, Y., Schaller, M.D., and Eck, M.J. (2007). Structural basis for the autoinhibition of focal adhesion kinase. Cell *129*, 1177–1187.

Lindauer, K., Loerting, T., Liedl, K.R., and Kroemer, R.T. (2001). Prediction of the structure of human Janus kinase 2 (JAK2) comprising the two carboxy-terminal domains reveals a mechanism for autoregulation. Protein Eng. *14*, 27–37.

Lucet, I.S., Fantino, E., Styles, M., Bamert, R., Patel, O., Broughton, S.E., Walter, M., Burns, C.J., Treutlein, H., Wilks, A.F., and Rossjohn, J. (2006). The structural basis of Janus kinase 2 inhibition by a potent and specific pan-Janus kinase inhibitor. Blood *107*, 176–183.

Matadeen, R., Hon, W.C., Heath, J.K., Jones, E.Y., and Fuller, S. (2007). The dynamics of signal triggering in a gp130-receptor complex. Structure *15*, 441–448.

Murakami, M., Narazaki, M., Hibi, M., Yawata, H., Yasukawa, K., Hamaguchi, K., Taga, T., and Kishimoto, T. (1991). Critical cytoplasmic region of the interleukin-6 signal transducer gp130 is conserved in the cytokine receptor family. Proc. Natl. Acad. Sci. USA *88*, 11349–11353.

Ohi, M., Li, Y., Cheng, Y., and Walz, T. (2004). Negative staining and image classification—powerful tools in modern electron microscopy. Biol. Proced. Online *6*, 23–34.

Pettersen, E.F., Goddard, T.D., Huang, C.C., Couch, G.S., Greenblatt, D.M., Meng, E.C., and Ferrin, T.E. (2004). UCSF Chimera–a visualization system for exploratory research and analysis. J. Comput. Chem. *25*, 1605–1612.

Radermacher, M., Wagenknecht, T., Verschoor, A., and Frank, J. (1987). Three-dimensional reconstruction from a single-exposure, random conical tilt series applied to the 50S ribosomal subunit of Escherichia coli. J. Microsc. *146*, 113–136.

Ritchie, T.K., Grinkova, Y.V., Bayburt, T.H., Denisov, I.G., Zolnerciks, J.K., Atkins, W.M., and Sligar, S.G. (2009). Chapter 11 - Reconstitution of membrane proteins in phospholipid bilayer nanodiscs. Methods Enzymol. *464*, 211–231.

Saharinen, P., and Silvennoinen, O. (2002). The pseudokinase domain is required for suppression of basal activity of Jak2 and Jak3 tyrosine kinases and for cytokine-inducible activation of signal transduction. J. Biol. Chem. *277*, 47954–47963.

Schindler, C., Levy, D.E., and Decker, T. (2007). JAK-STAT signaling: from interferons to cytokines. J. Biol. Chem. *282*, 20059–20063.

Seubert, N., Royer, Y., Staerk, J., Kubatzky, K.F., Moucadel, V., Krishnakumar, S., Smith, S.O., and Constantinescu, S.N. (2003). Active and inactive orientations of the transmembrane and cytosolic domains of the erythropoietin receptor dimer. Mol. Cell *12*, 1239–1250.

Skiniotis, G., Boulanger, M.J., Garcia, K.C., and Walz, T. (2005). Signaling conformations of the tall cytokine receptor gp130 when in complex with IL-6 and IL-6 receptor. Nat. Struct. Mol. Biol. *12*, 545–551.

Skiniotis, G., Lupardus, P.J., Martick, M., Walz, T., and Garcia, K.C. (2008). Structural organization of a full-length gp130/LIF-R cytokine receptor transmembrane complex. Mol. Cell *31*, 737–748.

Stewart, A., and Grigorieff, N. (2004). Noise bias in the refinement of structures derived from single particles. Ultramicroscopy *102*, 67–84.

Stroud, R.M., and Wells, J.A. (2004). Mechanistic diversity of cytokine receptor signaling across cell membranes. Sci. STKE *2004*, re7.

Wang, X., Lupardus, P., Laporte, S.L., and Garcia, K.C. (2009). Structural biology of shared cytokine receptors. Annu. Rev. Immunol. *27*, 29–60.

Williams, N.K., Bamert, R.S., Patel, O., Wang, C., Walden, P.M., Wilks, A.F., Fantino, E., Rossjohn, J., and Lucet, I.S. (2009). Dissecting specificity in the Janus kinases: the structures of JAK-specific inhibitors complexed to the JAK1 and JAK2 protein tyrosine kinase domains. J. Mol. Biol. *387*, 219–232.

Xu, Y., Kershaw, N.J., Luo, C.S., Soo, P., Pocock, M.J., Czabotar, P.E., Hilton, D.J., Nicola, N.A., Garrett, T.P., and Zhang, J.G. (2010). Crystal structure of the entire ectodomain of GP130: insights into the molecular assembly of the tall cytokine receptor complexes. J. Biol. Chem. *285*, 21214–21218.

Zhou, Y.J., Chen, M., Cusack, N.A., Kimmel, L.H., Magnuson, K.S., Boyd, J.G., Lin, W., Roberts, J.L., Lengi, A., Buckley, R.H., et al. (2001). Unexpected effects of FERM domain mutations on catalytic activity of Jak3: structural implication for Janus kinases. Mol. Cell *8*, 959–969.

Structure
Article

Structural Snapshots of Full-Length Jak1, a Transmembrane gp130/IL-6/IL-6Rα Cytokine Receptor Complex, and the Receptor-Jak1 Holocomplex

Patrick J. Lupardus,[1,6] Georgios Skiniotis,[2,5,6] Amanda J. Rice,[2] Christoph Thomas,[1] Suzanne Fischer,[1] Thomas Walz,[2,3] and K. Christopher Garcia[1,4,*]
[1]Departments of Molecular and Cellular Physiology and Structural Biology, Stanford University School of Medicine, Stanford, CA 94305, USA
[2]Department of Cell Biology
[3]Howard Hughes Medical Institute
Harvard Medical School, 240 Longwood Avenue, Boston, MA 02115, USA
[4]Howard Hughes Medical Institute, Stanford University School of Medicine, Stanford, CA 94305, USA
[5]Present address: Life Sciences Institute & Department of Biological Chemistry, University of Michigan Medical School, Ann Arbor, MI, 48109, USA
[6]These authors contributed equally to this work
*Correspondence: kcgarcia@stanford.edu
DOI 10.1016/j.str.2010.10.010

SUMMARY

The shared cytokine receptor gp130 signals as a homodimer or heterodimer through activation of Janus kinases (Jaks) associated with the receptor intracellular domains. Here, we reconstitute, in parts and whole, the full-length gp130 homodimer in complex with the cytokine interleukin-6 (IL-6), its alpha receptor (IL-6Rα) and Jak1, for electron microscopy imaging. We find that the full-length gp130 homodimer complex has intimate interactions between the trans- and juxtamembrane segments of the two receptors, appearing to form a continuous connection between the extra- and intracellular regions. 2D averages and 3D reconstructions of full-length Jak1 reveal a three lobed structure comprising FERM-SH2, pseudokinase, and kinase modules possessing extensive intersegmental flexibility that likely facilitates allosteric activation. Single-particle imaging of the gp130/IL-6/IL-6Rα/Jak1 holocomplex shows Jak1 associated with the membrane proximal intracellular regions of gp130, abutting the would-be inner leaflet of the cell membrane. Jak1 association with gp130 is enhanced by the presence of a membrane environment.

INTRODUCTION

Cytokine-induced homo- or heterodimerization of cell surface receptors is a ubiquitous signaling paradigm in higher eukaryotes (Stroud and Wells, 2004; Wang et al., 2009). Cytokines of the four helix bundle family are required for the growth and differentiation of nearly all cell types, but are particularly important for regulation of the immune and hematopoietic systems. Activation of signaling involves homo- or heterodimerization of two receptors by a single cytokine molecule, as first illustrated by Human Growth Hormone (HGH) in complex with its receptor (HGH-R) (de Vos et al., 1992). This dimerization event initiates activation of Janus kinases (Jaks) that are bound to the intracellular domains of the receptors (Ihle, 1995). The active kinases then phosphorylate the C-terminal intracellular tails of the receptors on specific tyrosine residues, creating binding sites for pathway-associated signaling molecules such as STAT (signal transducer and activator of transcription) transcription factors which, upon phosphorylation by the active Jaks, translocate to the nucleus where they activate transcription of cytokine-responsive genes (Leonard and O'Shea, 1998).

Gp130 serves as a shared signaling receptor for at least eight different cytokines, including IL-6, IL-11, IL-27, Leukemia Inhibitory Factor (LIF), Oncostatin-M (OSM), Ciliary Neurotrophic Factor (CNTF), Cardiotrophin-1 (CT-1), and Cardiotrophin-like-cytokine (CLC) (Bravo and Heath, 2000; Wang et al., 2009). Gp130 has evolved a remarkable set of structural characteristics to facilitate shared signaling. First, gp130 has evolved cross-reactive cytokine binding sites that are structurally ideal for engaging a highly varied set of cytokines either alone (LIF, OSM) or with associated alpha receptor subunits (IL-6, IL-11, CNTF, CT-1, CLC) (Boulanger et al., 2003a; Boulanger and Garcia, 2004). Second, gp130 can homodimerize or heterodimerize with a second gp130 family receptor (LIFR, OSMR, TCCR) depending on the cytokine encountered (Heinrich et al., 2003).

Homodimerization of gp130, which occurs in response to the cytokines IL-6 and IL-11, occurs in a three step fashion, with the cytokine first binding to the ligand-specific alpha receptor (site 1), followed by binding to gp130 to form the signaling-competent hexamer (Boulanger et al., 2003b; Chow et al., 2001) that comprises the membrane-distal "headpiece" and membrane-proximal "legs" (Figure 1A). An electron microscopy (EM) study of the complete extracellular domains of gp130 bound to IL6/IL6-Rα indicated a convergence of the membrane proximal D6 "leg" domains of gp130 (Skiniotis et al., 2005). This finding was supported by a cryoelectron microscopic study of the IL-11/IL-11Rα/gp130 complex, where the legs also appeared to converge in a ring-like shape (Matadeen et al., 2007). A subsequent EM study on the full-length gp130/LIF-R/CNTF

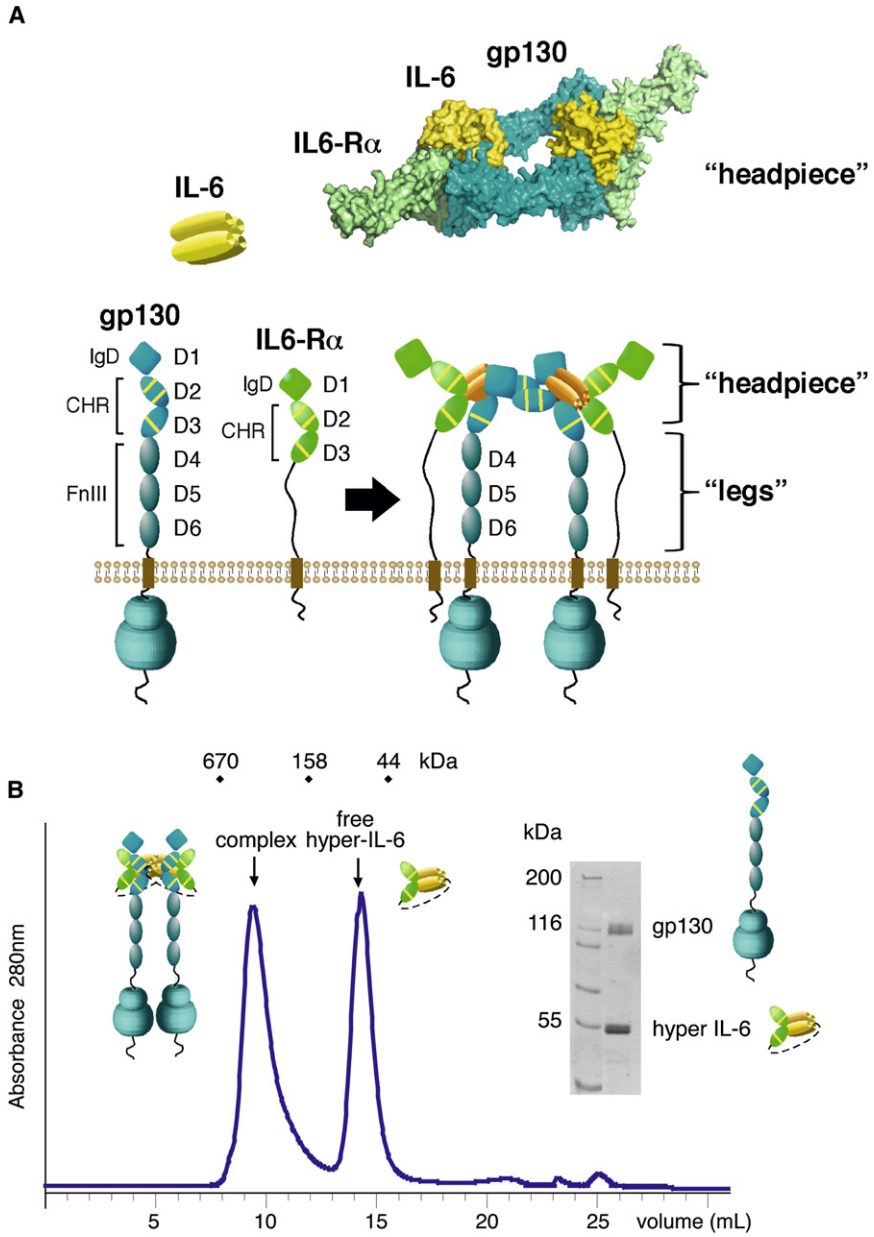

Figure 1. Assembly and Purification of the Full-Length gp130/IL-6/IL-6Rα Complex

(A) Components of the gp130/IL-6/IL-6Rα complex in pre- and postassembly state. A surface rendering of the structure of the signaling hexamer is shown on top. IgD denotes Ig-like domain, CHR denotes cytokine-binding homology region, and FnIII denotes Fibronectin-type III domain.

(B) Purification of the gp130/ IL6/IL6Rα complex by size exclusion chromatography.

complex, containing the TM segments and intracellular domains (ICDs), revealed a surprisingly intimate interaction between the extracellular juxtamembrane domains of gp130 and LIF-R (Skiniotis et al., 2008). Finally, a recent crystal structure of a complete, but unliganded, gp130 extracellular domain showed that, consistent with the EM studies, the gp130 legs are kinked at the D4-D5 boundary, and as a result would bend inward toward one another within the dimeric complex (Xu et al., 2010).

A critical piece of the puzzle to understand cytokine receptor signaling involves the Jak/Tyk family of intracellular kinases, which have remained enigmatic structurally (Leonard and O'Shea, 1998; Schindler et al., 2007). The Jak/Tyk family consists of four members, Jak1, Jak2, Jak3, and Tyk2, that are associated with cytokine receptors through a small membrane-proximal region of the ICD called the "Box 1/Box 2" (Haan et al., 2006; Murakami et al., 1991). The Jaks are ~1200 amino acid proteins that are subdivided by sequence into seven Janus homology regions (JH1-7) which fold into four distinct domains (Haan et al., 2006). The N terminus consists of a FERM domain, which mediates the interaction with cytokine receptors, followed by an SH2-like domain and a pseudokinase domain that lacks catalytic activity, and finally the C terminus is the active tyrosine kinase domain (KD). Several publications have suggested that Jak activation is regulated through interdomain communication, such as between the FERM and KD, requiring conformational change during signaling (Zhou et al., 2001). Further, disease-related mutations in Jaks have been speculated to interfere with the ability of Jak to undergo normal allosteric regulation (Funakoshi-Tago et al., 2008; Zhou et al., 2001). However, although several isolated KD structures have been reported (Boggon et al., 2005; Chrencik et al., 2010; Lucet et al., 2006), little is known about the structure of intact Jak family members.

In this study, we capitalize on the characteristic shape of the "tall" gp130 extracellular regions to visualize the full-length receptor holocomplex by single particle EM. We reconstitute and image a receptor signaling complex including IL-6, IL-6Rα, gp130, and Jak1, both in isolation, and in complex with each other. The EM images indicate that the full-length gp130/IL-6/IL-6Rα ternary complex forms a well-defined, structurally stabilized assembly with the juxtamembrane and transmembrane domains in intimate contact upon ligand binding. Projection averages and reconstructions of Jak1 show it to be a three-lobed molecule with conformational flexibility that could, in principle, facilitate interdomain communication. The holocomplex images suggest that homodimerization of gp130 by IL-6 locks the extracellular/transmembrane domains of gp130 together into continuous unit that can sensitively transduce a conformational signal through the plasma membrane to Jaks that are bound at the extreme juxtamembrane

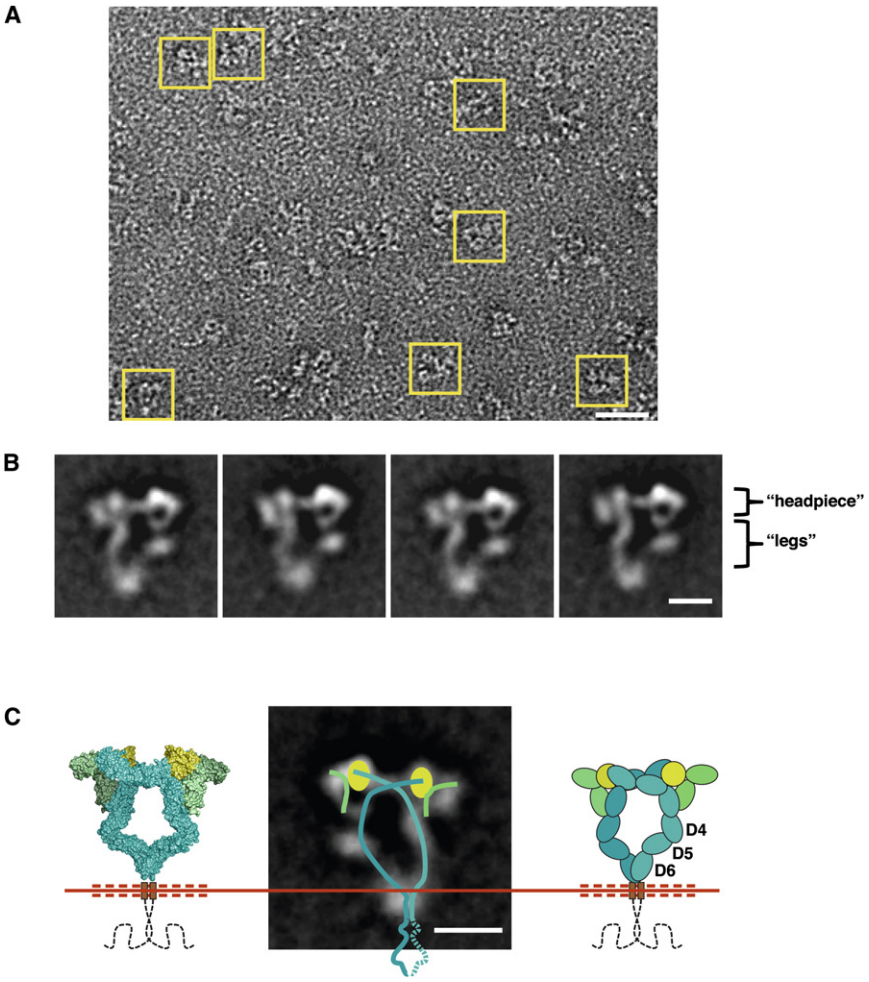

Figure 2. 2D EM Averages of the Full-Length gp130/IL-6/IL-6Rα Complex

(A) Raw image of negatively stained full-length gp130/IL-6/IL-6Rα complexes. Representative particles are boxed in yellow.

(B) 2D class averages of the gp130/hyper IL-6 complex produced by the classification of 6070 particles.

(C) Comparison of a 2D class average to a model based on the gp130/IL-6Rα/IL-6 complex (left). The cartoon on the right shows the domain organization of the gp130/ IL-6Rα/IL-6 complex. Lines overlaid on the 2D average trace the chains of the receptors and denote the location of the IL-6 cytokine.

Scale bars in (A) and (B) and (C) correspond to 40 and 10 nm, respectively.

See also Figure S1.

regions of the intracellular domains, likely interacting with the inner leaflet of the cell membrane.

RESULTS

Imaging the gp130/IL-6/IL-6Rα Transmembrane Complex

We took advantage of the highly characteristic and extended structure of gp130, which as a "tall" receptor has six extracellular domains, compared with two or three for most cytokine receptors, to attempt EM imaging of the full-length receptor (Figure 1A). The extracellular complex structure is a roughly triangular assembly containing the membrane-distal ligand binding "headpiece" and membrane-proximal "legs," and these obvious features serve as clear fiducial landmarks for particle identification on EM grids. As a prerequisite to reconstituting a complete IL-6/IL-6Rα/gp130/Jak1 quaternary signaling complex, we first purified and characterized the full-length ternary complex between IL-6, IL-6Rα, and gp130 in order to produce comparison images of the receptor complex with and without Jak1 included.

We expressed full-length gp130 in insect cells, with a C-terminal antibody epitope tag (EYMPME) and solubilized the receptor in the detergent n-dodecyl-β,D-maltoside (DDM). Gp130 was then captured from the detergent solubilized membranes by a Glu-Glu antibody affinity column and competitively eluted with soluble peptide. The eluate was then incubated with an excess of soluble IL-6/IL-6Rα fusion protein (also termed "hyper-IL6"; Fischer et al., 1997) to form the dimerized ternary complex (i.e., the hexamer), and further purified by size exclusion chromatography (Figure 1B). The complex was very stable and eluted from the column as a single peak of ~400 kDa, which is the approximate size of two receptors (2 × 110 kDa) and two hyper-IL-6 molecules (2 × 55 kDa), allowing ~90 kDa for the detergent micelle.

We then employed EM to visualize the complexes embedded in negative stain, which revealed monodisperse particles of similar size and shape (Figure 2A). Classification of 6070 particles (from 56 images taken on film) into 15 classes produced class averages that showed a dominant preferred particle orientation on the carbon support (see Figure S1 available online). As we have previously observed in the case of the extracellular gp130 complex (Skiniotis et al., 2005), the class averages of the full-length gp130 complex reveal a characteristic pseudo-two-fold symmetric particle, in which the gp130 leg domains (D4-D6) project from the cytokine binding headpiece containing IL-6 and IL-6Rα, and subsequently bend toward each other before joining at the their C-terminal tips at the level of the TM segments (Figures 2B and 2C). Strikingly, in contrast to the leg flexibility observed in the complex that contained only the extracellular domains of gp130 (Skiniotis et al., 2005), the class averages of the full-length gp130 complex containing TM segments indicate a conformationally rigid particle with uniform closure of the gp130 membrane-proximal domains (Figure 5, compare top and middle panels). The 2D averages here show homogenous leg positioning, with the D6 and transmembrane domains

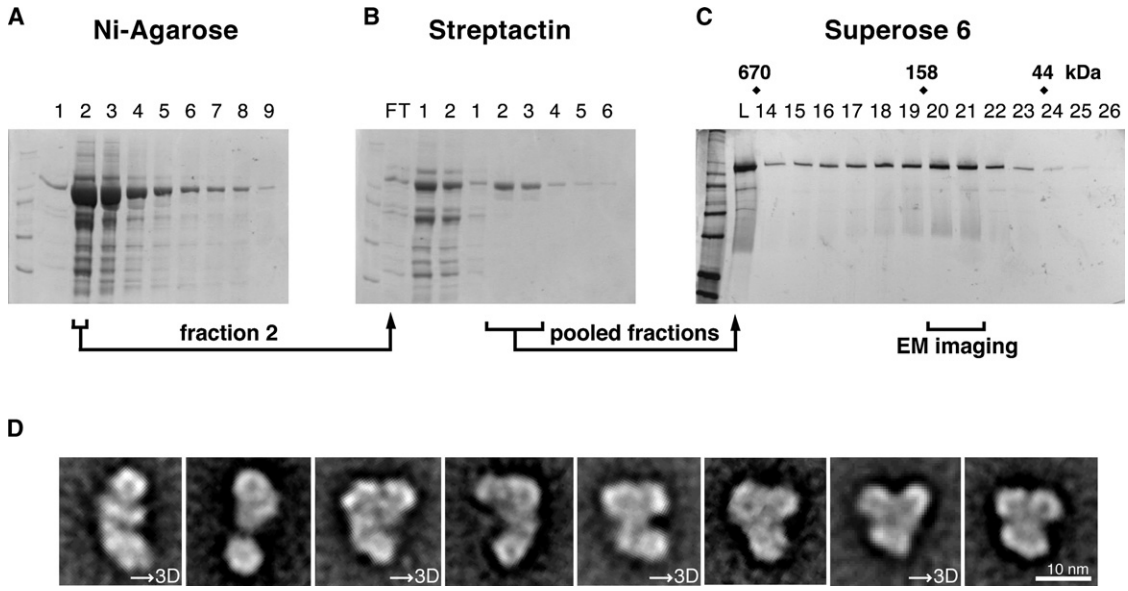

Figure 3. Purification and 2D Projections of Recombinant Human Jak1

(A) Jak1 was expressed using the BacMam system, and purified from 293S cell lysate via a C-terminal 8-Histidine tag using Ni-affinity column.

(B) Second step, streptactin-affinity purification of Jak1 via its N-terminal Strep-tag.

(C) Silver-stained gel of Streptactin-purified Jak1 after a Superose 6 size exclusion chromatography step. These fractions were selected for negative stain EM. See Figure S2.

(D) Representative 2D class averages of purified Jak1 obtained from the classification of 9258 particles. The marked classes were used independently for 3D reconstructions.

See also Figures S3–S5.

closely apposed. The presence of the TM segments in the complex may possibly stabilize the leg closure of gp130, as cytokine receptor TM helices have been proposed to self-associate within the membrane (Constantinescu et al., 2001; Kubatzky et al., 2001). Below the TM regions, little density was visible, indicating the intracellular domains of the gp130 homodimeric complex are loosely structured as seen in the gp130/LIFR heterodimeric complex (Skiniotis et al., 2008).

Purification and Imaging of Jak1

To generate sufficient quantities of Jak1 for imaging studies, we used the BacMam system and 293S cells (Figure 3; Dukkipati et al., 2008). Prior efforts to produce a variety of different full-length Jak molecules in insect cells resulted in aggregated and inactive material. The material from 293S cells is soluble, although it is not amenable to high protein concentrations, and solubility is enhanced by the presence of detergent (0.01% DDM). We utilized a three step purification scheme to purify Jak1 to >98% purity (Figures 3A–3C). Jak1 was first purified via a C-terminal 8-Histidine tag from 4 liters of 293S cell lysate using Nickel-agarose (Figure 3A), followed by Streptactin purification via an N-terminal Strep-tag (Figure 3B). The protein was then purified by size exclusion chromatography on Superose 6 to generate monodisperse Jak1 for EM imaging (Figure 3C). While the gel filtration elution peak was broad, a significant fraction of the material eluted at a position expected for monomeric Jak1. Additionally, the recombinant Jak1 we purified from mammalian cells was active at phosporylating the gp130 intracellular domain in kinase assays (Figure S2).

We again employed negative stain EM to visualize our preparations of Jak1 (Figure 3D). Raw images of Jak1 indicated a monodisperse particle population, albeit with a high degree of conformational variability (Figure S3). To analyze these conformers we interactively selected 24,356 particle pairs and used image classification to select the most consistent 9258 particles (Figure S4; see Experimental Procedures). After classification of the 9258 particles from the images of the untilted specimens into 50 classes (Figure S5), the resulting 2D class averages of Jak1 (representative 2D averages shown in Figure 3D) confirmed our suspicion of a highly flexible particle ranging from an extended to a compact conformation. In the class averages we can discern three main lobe densities, two in constant close proximity, and a third more globular, larger one in variable positions.

3D Reconstruction of Jak1

To gain further insight to the conformations presented by Jak1, and considering the high level of conformational variability observed, we used the corresponding particles selected from images of the tilted specimens to calculate separate 3D reconstructions for individual classes (containing from 446 to 1050 particles) produced by 2D classification (Figure 3D; Figure S5). While there are many classes evident, we focused our approach on three well-defined classes that exemplify intermediates in a transition from a fully extended to a compact conformation, as shown in Figure 4 (top panel-open to bottom panel-closed). 3D reconstructions were initially calculated by back-projection according to the random conical tilt method (Radermacher

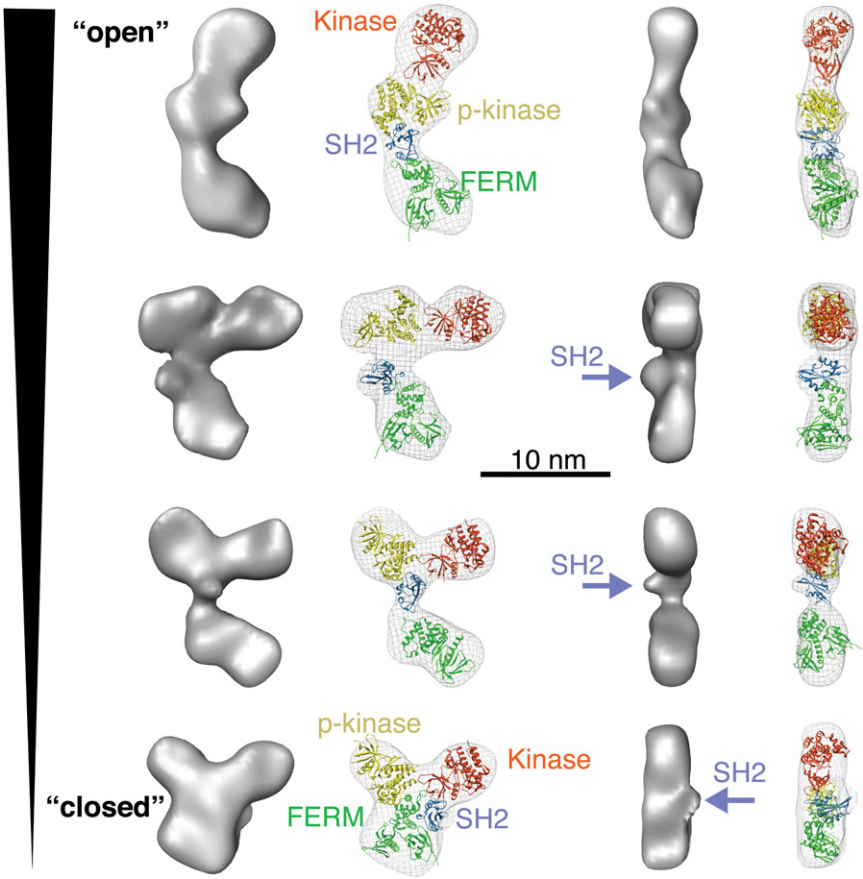

Figure 4. 3D Reconstructions and Modeling of Full-Length Human Jak1

3D reconstructions of Jak1 are based on individual classes obtained from 2D classification of untilted specimen projections (marked in Figure 3D and Figure S6). From the top to the bottom of the panel Jak1 particles transition from open to closed conformations. The FERM (green), SH2-like (cyan), pseudokinase (yellow), and kinase (red) domains of Jak1 were modeled into the EM densities. The orientations of the reconstructions in the left column of the panel are viewing the particles "face-on" the grid (as shown in the 2D class averages of Figure 3D), while the orientations to the right are rotated 90°, reflecting the flatness of the surface on which Jak1 is lying.
See also Figures S5 and S6.

et al., 1987) and further refined after the inclusion of 0° particle projections. The resulting 3D models at a resolution of ~35 Å (as judged by Fourier shell correlation) (Figure S6) reveal a highly asymmetric molecule displaying three major lobes (Figure 4). As also indicated in the 2D class averages (Figure 3D), two of the major lobes are always in close proximity, in what appear to be extended "longitudinal" interactions. In contrast, the third lobe appears as an individually larger, more globular domain that is loosely connected to the first two modules, thereby adopting variable positions with respect to the other two lobes. Interestingly, with the exception of the fully extended conformation ("open"), all reconstructions display an additional minor lobe, or "bump," which projects between the globular mobile and the two stable lobes, that is most likely the SH2 domain (indicated by arrows in Figure 4).

In order to interpret the densities revealed in our reconstructions we manually fit models of appropriate domains from available crystal structures into the density maps. To model the kinase and pseudokinase domains, we used two copies of the atomic resolution structure of the Jak1 kinase domain (PDB ID: 3EYH) (Chrencik et al., 2010). We used homologous crystal structures for the Focal Adhesion Kinase FERM domain (PDB ID: 2AL6) (Ceccarelli et al., 2006) and the Src SH2 domain (PDB ID: 1IJR) (Kawahata et al., 2001). Sequence comparisons indicate that the interdomain linker connecting the FERM-SH2 module with the pseudokinase module is approximately 20 amino acids long. Thus we reasoned that the larger globular lobe, loosely connected at one end of the EM density should correspond to the FERM domain, which appears to fit well in that position (Figure 4). In a next step, we modeled the SH2 domain at the border region between the FERM domain and two stable major lobes, thereby occupying the minor lobe shown in our 3D reconstructions. Subsequently, we docked the pseudokinase domain within the middle major lobe, which is immediately adjacent to the FERM-SH2 module, followed by the C-terminal kinase domain (KD). The 3D maps lack sufficient resolution to propose specific interactions between the individual domains of Jak1. However, our density maps and modeling argue that the FERM-SH2 module adopts variable conformations in relation to the pseudokinase-kinase module, and this is consistent with sequence analysis that indicates a longer linker between the FERM-SH2 and pseudokinase domains. In the compact Jak1 conformation, the close proximity of the FERM-SH2 module to the catalytic KD supports the possibility of a direct interaction as has been suggested by earlier biochemical studies (Funakoshi-Tago et al., 2008; Zhou et al., 2001), and analogous to that seen for Focal Adhesion Kinase (discussed later) (Lietha et al., 2007).

Preparation and Imaging of the gp130/IL-6/IL-6Rα/Jak1 Complex

To prepare the quaternary gp130/IL-6/IL-6Rα/Jak1 complex, purifications of the ternary gp130/IL-6/IL-6Rα complex and Jak1 were carried out concurrently. The gp130 complex was mixed with Jak1 purified from Streptactin, incubated overnight, and further purified by either anion exchange (Mono-Q) (Figure 5A) or size exclusion chromatography. Jak1 alone does not adhere strongly to mono-Q, but co-elutes as a complex with the receptor, although there is some dissociation during purification since the interaction does not appear to be high affinity. Raw EM images of our gp130/IL-6/IL-6Rα/Jak1 complex preparations in negative stain showed a significant fraction of bulkier

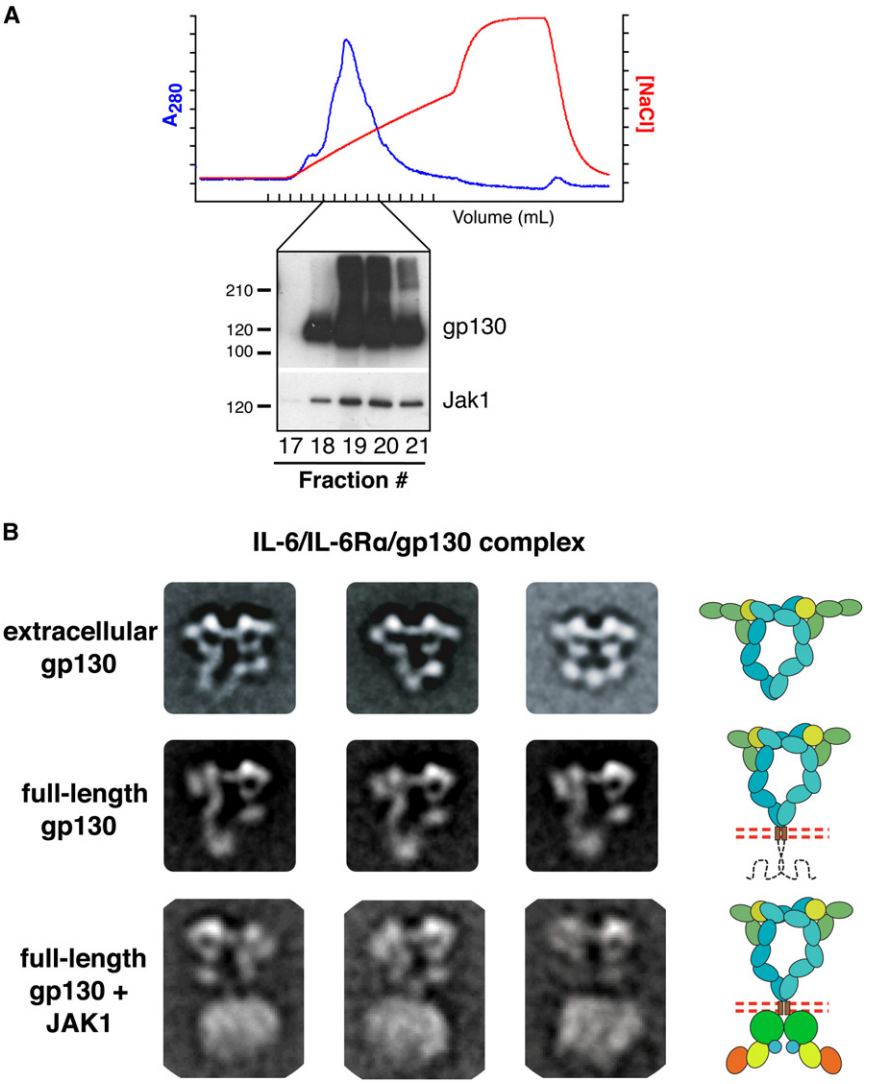

Figure 5. Purification and EM Imaging of the gp130/IL-6/IL-6Rα/Jak1 Complex

(A) Anion-exchange chromatography of the gp130/Jak1 complex. Fractions from the Mono-Q column were analyzed by SDS-PAGE gel and western blot with anti-GluGlu (gp130) and anti-Jak1 antibodies (panel underneath). Since two different antibodies were used to detect gp130 (Anti-GluGlu) and Jak1 (Anti-Jak1) the relative ratios of gp130/Jak1 cannot be derived from this experiment. The anti-GluGlu mAb appears to be more sensitive than anti-Jak1.

(B) Comparison of representative 2D averages for the soluble gp130/IL-6/IL-6Rα extracellular complex (top three panels), full-length gp130/IL-6/IL-6Rα (middle panels, as shown in Figure 2B), and the gp130/IL-6/IL-6Rα/Jak1 complex (bottom three panels). Schematics for each complex are shown in the far right column. The extra fuzzy density in the Jak1 loaded complexes is apparent by comparison to the non-loaded complexes. See also Figures S7 and S8.

particles when compared to full-length receptor in the absence of Jak1 (Figure S7). We were able to easily discern the characteristic side views of the extracellular domains and headpiece, as seen in the soluble and full-length receptor complex EM images not containing Jak1, with significant additional mass following the membrane proximal FNIII legs and TM regions (Figure 5B, bottom row). We selected 14,008 particles from 224 images taken on imaging plates, of which 3975 particles (see Materials and Methods) were used for the final classification into 30 classes (Figure S8). Most of the resulting class averages show the clear pseudo-two-fold symmetric densities representing the extracellular regions of the receptor complex (representative class averages shown in Figure 5B, bottom panels). Directly below the transmembrane level we observe additional density that can only represent the bound Jak1. In fact, direct comparison of the "unloaded" gp130/IL-6/IL-6Rα ternary complex to that "loaded" with Jak1 clearly shows its position (compare Figure 5B middle and bottom rows). However, the Jak1 densities appear "fuzzy" and are not well resolved. This is likely due to variability in the Jak1 molecule conformations, and also variable orientations of Jak1 on the carbon support. This conformational mixture is probably also amplified by the flexible nature of the gp130 intracellular domains to which Jak1 is bound. Nevertheless, Jak1 appears to bind near the base of the TM region, at the extreme membrane proximal region of the gp130 ICD, where its binding site has been mapped (Haan et al., 2002).

Given the apparent "free swinging" of the Jak1/ICD module underneath the TM segment in the detergent-solubilized receptor complex, and the proximity of the inner leaflet of the membrane bilayer in the cell, we were curious if the addition of a bilayer environment might stabilize the Jak1 interaction. Therefore we reconstituted gp130/IL-6/IL-6Rα complexes in nanodiscs, which provide a bilayer surrounding the TM region (Figure 6). The nanodisc reconstitution was highly efficient for the gp130 complex using the MSP-1 protein and lipid to displace the detergent micelle. We were able to purify the ternary complex by gel filtration in the absence of detergent. We then added purified recombinant Jak1 to the gp130/IL-6/IL-6Rα nanodisc, and subjected the mixture to gel filtration (Figure 6). We found that the association of Jak1 with gp130 was far more stable and efficient than in detergent micelles (Figure 5), and the resultant holocomplex could be purified in nearly a stoichiometric ratio, with little Jak1 dissociation.

DISCUSSION

Our mechanistic understanding of communication between cytokine recognition and intracellular Jak/Tyk activation is poor compared to systems such as receptor Tyrosine Kinase's

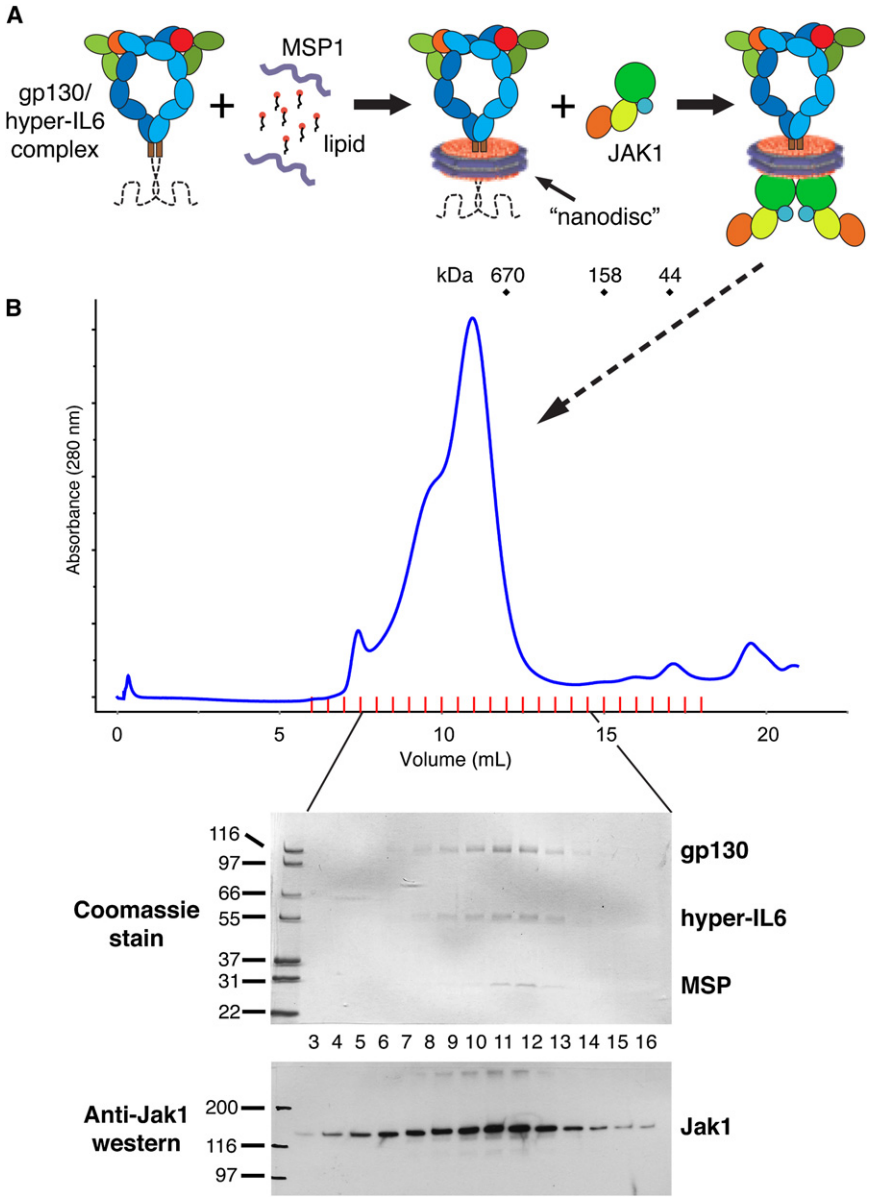

Figure 6. Reconstitution of the gp130/IL-6/IL-6Rα/Jak1 Complex in Lipid Nanodiscs

(A) The quaternary gp130/IL-6/IL-6Rα/Jak1 complex was prepared and incorporated into lipid "nanodiscs" comprising DPPC and the MSP1 scaffold protein, and purified by gel filtration chromatography (Superose 6) in the absence of detergent.

(B) Jak1 was then added to the nanodiscs containing gp130/ gp130/IL-6/IL-6Rα and again applied to a Superose 6 size exclusion column. Since full-length Jak1 and gp130 comigrate on SDS-PAGE, peak fractions were subjected to SDS-PAGE and Coomassie staining (top panel) and western blotting with an anti-Jak1 antibody (bottom panel) in order to confirm the presence of both components. Higher resolution SDS-PAGE and Coomassie confirms that both proteins are present in roughly equal amounts.

(RTK's), and Death receptors. The principal challenges to making progress on this problem have been the historic recalcitrance of Jak expression, and the difficulties posed by intact single-pass TM receptors for structural studies. Our strategy was to produce full-length Jak1 for EM analysis both alone and in complex with full-length gp130, and this has enabled us to report the first structural snapshots of Jak1, as well as of a fully "loaded" transmembrane receptor complex. While the mechanistic insight that can be gained from our studies is limited, the results we show here are informative on several levels. Our choice of gp130 was driven by its very characteristic extracellular structure by single-particle EM, which allows us to rapidly identify and orient particles. These studies demonstrate imaging of the cytokine receptor holocomplex is technically feasible, and that higher resolution imaging methodologies combined with nanodisc stabilization could lead to deeper mechanistic insights.

Imaging of the gp130/IL-6/IL-6Rα Complex

Two previous single-particle EM studies of gp130 complexes with IL-6 and IL-11, respectively, included only the extracellular domains of gp130 (Matadeen et al., 2007; Skiniotis et al., 2005). In the gp130/IL-6/IL-6Rα study, the majority of particles showed the gp130 leg domains together at the level of the membrane, but a number of other "open" conformations were observed, indicating that the leg domains were not necessarily holding the transmembrane domains together. In the IL-11/IL-11Rα/gp130 ectodomain complex, normal-mode analysis of the ring-like structure indicated a high degree of conformational flexibility in the leg regions that was speculated to facilitate rearrangement during signaling. In the current study, we observe that when the transmembrane and intracellular domains are included, the gp130 leg domains uniformly converge at the level of the membrane, and form an apparently continuous, possibly rigidified unit together with the transmembrane segments. This interaction is consistent with functional data suggesting critical interactions between the membrane proximal domains of gp130, where antagonistic antibodies map to the D4-D6 region of gp130 (Kurth et al., 2000). Association of the TM regions is also in accord with studies on EPO and Prolactin receptors showing the TM helix packing interactions within cytokine receptor dimers may be prevalent (Constantinescu et al., 2001; Kubatzky et al., 2001). Our prior EM imaging studies of the heterocomplex of full-length gp130 and LIF-R in complex with CNTF/CNTF-Rα, also indicated that the leg and TM domains were intimately associated upon ligand binding (Skiniotis et al., 2008).

The gp130 leg domains are "kinked" near the D4-D5-D6 boundaries, forcing the trajectory of the legs toward the center of the complex, enabling the juxtamembrane and transmembrane domains to be in close proximity. Indeed, a kink is also observed in this region of the D5 domain of gp130 in the gp130/LIFR/CNTF/CNTF-Rα complex (Skiniotis et al., 2008), and an acute bend between the D4 and D5 domains is observed in the crystal structure of the entire gp130 extracellular domain (Xu et al., 2010). Thus, the compendium of gp130 structures, both crystallographic and EM, suggest that the gp130 legs are bent, and in intimate association within the active signaling complex. Although we cannot visualize the TM interactions in detail at the resolution of the EM analysis, the structural evidence suggests that the close association of the membrane proximal regions of the legs is most likely assisted by packing interactions between the TM helices within the dimer, forming a continuous unit between the extracellular juxtamembrane regions and the TM. Thus, this possible packing between the TM helices of cytokine receptor dimers may be a general means of rigidifying the linkage between extracellular cytokine recognition and intracellular signaling. Such a rod-like unit would facilitate the transmission of subtle receptor positional differences to the intracellular signaling components by propagating, rather than absorbing extracellular torque. A similar model has been previously proposed based on structure-function studies of the EPO receptor (Seubert et al., 2003).

Imaging of Jak1

Our current structural knowledge of the Jak/Tyk family is limited to the obvious homologies of individual domains to known folds, such as the FERM, SH2 and pseudokinase domains, and crystal structures of several Jak KD's, including Jak1. But it is important to structurally characterize a full-length Jak given the apparent interdomain communication required for activation. 2D class averages and 3D reconstructions of full-length Jak1 indicate that the four major subdomains fold into three modules: (1) the larger FERM module, (2) an extended pseudo-kinase and kinase module, and (3) a module consisting of a smaller domain between the lobes that is likely the SH2-like domain (Figure 4). It is clear from our analysis that the Jak1 subdomains are highly flexible with respect to one another, and can exist in wide array conformations ranging from open to closed. Our results also suggest that the kinase and pseudokinase subdomains are closely associated with one another, forming a rather continuous bi-lobed module. This configuration differs from the JH1-JH2 domain relationship predicted from a homology modeling study of Jak2 that was based on the FGF receptor kinase dimer structure (Lindauer et al., 2001). Several previous studies have suggested that regulation of the C-terminal KD takes place through its interactions with the N-terminal FERM domain, which would necessitate a compact state of Jak (Saharinen and Silvennoinen, 2002; Zhou et al., 2001). Coexpression of the isolated FERM domain with the isolated KD of Jak1, and deletion of the pseudokinase domain in Jak2 and Jak3, enhances KD activity. These findings suggest that: (1) the "active" form of Jak requires close proximity between the N- and C-terminal domains, and (2) a role of the pseudokinase domain may be to sterically interfere with Jak KD activation until receptor dimerization initiates a conformational change in Jak. Interestingly, in the compact Jak1 conformation we see by EM, the FERM and SH2 domains come in very close proximity to the catalytically active C-terminal KD, consistent with the biochemical studies (Zhou et al., 2001). Therefore, the built-in flexibility of Jak1 may facilitate regulation of KD activity by allowing Jak1 to shuttle between open and closed states. It was speculated recently that cytosolic Jak2 may be "locked" into an inactive compact state until its FERM domain engages the receptor (Funakoshi-Tago et al., 2008). Contrary to this model, our "free-floating" Jak1 reveals a highly diverse conformational ensemble relatively evenly dispersed between open and closed states, and partial open/closed states, that does not appear to be locked into a particular structure. However, we cannot say whether, or if, the open or closed conformations correspond to active or inactive Jak1. In order to address this, we have attempted to lock Jak1 into a compact state using linkers and other engineering approaches, but have so far been unsuccessful.

Focal Adhesion Kinase (FAK) has structural analogies to Jak/Tyk kinases, since FAK possesses an N-terminal FERM domain and a C-terminal KD. In the structure of autoinhibited FAK, the FERM and KD are in direct contact such that the FERM prevents access to the KD phosphorylation sites, whereas in the activated state, the FERM interaction is relieved (Lietha et al., 2007). Like FAK, Jak1 also possesses an N-terminal FERM and C-terminal KD that we see by EM exist in highly variable positions relative to one another, either in contact in the compact conformation, or far apart in the open conformation. The analogy to FAK suggests that the compact Jak1 conformation may represent an "inactive" conformation, in which the KD is autoinhibited by FERM interactions. However, unlike FAK, in Jak1 the FERM/KD interaction does not appear to be stable in solution in that the particles do not preferentially segregate into a close state. There is also the further consideration that FAK is a freely diffusing molecule within the cytosol, whereas Jak/Tyk proteins are primarily associated with cytokine receptors, which almost certainly influence Jak conformation. Thus, the receptor-bound form is, indeed, a more physiologically relevant state in which to image Jak, and this is where our efforts are directed.

The gp130/IL-6/IL-6Rα/Jak1 Complex

We prepared gp130/IL-6/IL-6Rα ternary complexes both in detergent micelles as well as in lipid "nanodiscs" that reconstitute a more physiological environment for transmembrane helices. Holocomplexes in detergent micelles were subjected to negative staining and EM imaging. The characteristic two-fold symmetric extracellular domains of gp130/IL-6/IL-6Rα are well resolved in the 2D averages. Below the TM region, a fuzzy density is observed that likely corresponds to bound Jak1 molecules, but the density cannot be fit with any Jak1 domains given its smeared character.

Imaging of the holocomplex denotes a proof-of-concept technical benchmark that requires substantial improvement before detailed structural conclusions can be reached. However several important facts have emerged from these experiments. First, our initial attempts to form complexes between Jak1 and an isolated soluble gp130 ICD were not successful, since the two components dissociated over gel filtration, indicating a very low affinity interaction (data not shown). Association of Jak1 with the full-length gp130 in detergent micelles was far

more efficient and lead to the isolation of complexes. Thus, the membrane/lipid environment appears to be important for Jak1 association with gp130 and by extension, perhaps, other cytokine receptors. Second, while Jak1 is present, it appears to exist as a conformational ensemble in the complex, as evidenced by the "fuzzy" density. We have previously shown that the gp130 intracellular domains are highly flexible, and not visible by 2D imaging (see Figure 2) (Skiniotis et al., 2008). The Box1/Box2 sequence region of gp130, to which the Jak1 FERM domain binds, is located at the extreme N-terminal region of the gp130 ICD (directly after the TM), and this is where we see the Jak1 density in the holocomplex. Presumably the uppermost part of the density corresponds to the FERM domains, while the density further away from the TM region of gp130 corresponds to the more C-terminal domains of Jak1 that are likely "free-swinging" since Jak1 is only bound to gp130 via its FERM. The nature of this single site Jak1-FERM/gp130 contact preserves the Jak1 interdomain flexibility that is likely necessary for the mechanism of Jak1 activation. The KD can, in principle, associate with the FERM, and then once activated, analogous to an unfolding scorpion's tail, phosphorylate STAT and other adaptors that are known to bind to the C-terminal regions of the gp130 ICD. Unfortunately, this flexibility prevents us from trapping the complex in a single position that will allow structural definitions to emerge. Therefore, these studies show that while it is indeed feasible to reconstitute the gp130 signaling holocomplex, future attempts will need to address the positional variability of the Jak/ICD module.

The holocomplex is greatly stabilized in nanodiscs, which provide a surrogate membrane bilayer. Our speculation is that the inner leaflet of the nanodisc is in contact with the Jak1 FERM domain that is bound to the Box1/Box2 near the membrane, stabilizing the interaction. The size of the FERM domain, coupled with the close proximity of the Box1/Box2 region to the TM segments of cytokine receptors, makes this a plausible scenario, especially considering the fact that our recombinant Jaks seem to require detergent for stability. Perhaps the FERM possesses a hydrophobic patch that is in contact with the membrane. Future attempts to visualize the gp130/Jak1 holocomplex will focus on cryoelectron microscopy of nanodisc-reconstituted complex.

EXPERIMENTAL PROCEDURES

Expression and Purification of the gp130/IL-6/IL-6Rα Complex

Full-length gp130 was expressed as previously described (Skiniotis et al., 2008). In brief, full-length, EYMPME-tagged gp130 was expressed in HiFive cells, cell membranes were isolated and solubilized in 1% n-dodecyl-β-d-maltoside (DDM), and recombinant receptors were purified via an anti-Glu-Glu-sepharose column. A soluble construct of human IL-6 fused to the D2-D3 cytokine binding region of IL-6Rα (hyper IL-6) (Fischer et al., 1997) was expressed and purified from HiFive cell supernatant via Ni-affinity and gel filtration chromatography. An excess of hyper-IL-6 was added to the purified gp130 and incubated overnight. The protein mixture was then concentrated and purified on a Superdex 200 column equilibrated in HEPES-buffered saline containing 100 μM DTT and 0.02% DDM.

Expression and Purification of Jak1

Full-length human Jak1 was cloned into the BacMam expression vector pVLAD6 (Dukkipati et al., 2008), and recombinant baculoviruses were prepared in SF9 insect cells. 293S cells were grown in suspension in Pro293 media (Lonza, Inc.), infected with Jak1 baculoviruses, and protein expressed for 24 hr at 37°C. Cells were pelleted, resuspended in buffer A (20 mM Tris-HCl [pH 8.0], 1 mM TCEP, and protease inhibitors) and dounce homogenized to lyse the cells. Insoluble material was pelleted at ~45,000 × g for 1 hr at 4°C, and the supernatant harvested. To the supernatant was added 500 mM NaCl, 0.1% DDM, 20 mM imidazole, and 5% glycerol, and the lysate was incubated with Ni-agarose affinity beads in batch for 2 hr. Beads were then collected and washed with buffer B (20 mM Tris-HCl [pH 8.0], 150 mM NaCl, 1 mM TCEP, 0.02% DDM, 5% glycerol) containing 20 mM imidazole, followed by elution of Jak1 from the beads in buffer B containing 200 mM imidazole. After nickel elution, Jak1 elutions were loaded onto a Streptactin-sepharose column, washed with buffer B, and eluted in buffer B containing 2.5 mM desthiobiotin. Following elution from the Streptactin column, NaCl and glycerol to 500 mM and 20% were added, respectively, in order to stabilize Jak1 in solution. Glycerol was dialyzed from the Jak1 fractions immediately prior to EM imaging. Detection of Jak1 was performed by Coomassie staining and by western blot with an anti-Jak1 antibody (BD Biosciences 610231). The kinase activity of purified Jak1 is described in Figure S2.

Electron Microscopy

Receptor complexes and Jak1 were prepared for electron microscopy using the conventional negative staining protocol (Ohi et al., 2004), and imaged at room temperature with a Tecnai T12 electron microscope operated at 120 kV using low-dose procedures. Images of the hyper-IL-6/gp130 complex were recorded on Kodak SO-163 film at a magnification of 52,000× and a defocus value of about −1.5 μm. Images of Jak1 and the hyper-IL-6/gp130/Jak1 complex were recorded on imaging plates (DITABIS, Digital Biomedical Imaging Systems AG) at a magnification of 67,000× and a defocus value of about −1.0 μm.

Image Processing

Film recorded micrographs were digitized with a Zeiss SCAI scanner using a step size of 7 mm, and 3 × 3 pixels were averaged to obtain a pixel size of 4.04 Å on the specimen level. Imaging plates were analyzed with a DITABIS micron plate reader, and 2 × 2 pixels were averaged to obtain a pixel size of 4.48 Å on the specimen level.

Multireference alignment and classification for the projection analysis of all samples was carried out using the SPIDER image processing suite (Frank et al., 1996).

For the 2D analysis of the gp130/IL-6/IL-6Rα transmembrane complex we interactively selected 6070 particles from 56 images taken on film. The particles were classified into 15 classes, producing consistent class averages that showed a dominant preferred particle orientation on the carbon support (Figure S1).

For 2D analysis and 3D reconstructions of Jak1 we interactively selected 24,356 particle pairs from 132 60°/0° image pairs taken on imaging plates. A first round of classification of the untilted specimen into 100 classes (Figure S4) revealed a substantial degree of conformational variability. As a result, several class averages were not well defined, either revealing particles of smaller size or particles that lacked distinct features. We thus selected the particles belonging to the better defined classes (marked with a green dot in Figure S4; total of 9258 particles), and subjected them to a second round of classification into 50 classes (Figure S5). Based on this second classification step, four independent 3D reconstructions were derived from 446 to 1050 particles belonging to single classes that revealed a range of JAK1 conformations, from fully extended ("open") to fully compact ("closed") (the classes used for 3D reconstruction are marked in Figure 3D and Figure S5). In brief, the random conical tilt technique (Radermacher et al., 1987) was used to calculate a first back projection map using the images of the tilted specimen. After angular refinement, the corresponding particles from the images of the untilted specimens were added and the images were subjected to another cycle of angular refinement. Using the resulting maps as reference models, we calculate final 3D reconstructions with the program FREALIGN (Stewart and Grigorieff, 2004). FREALIGN was also used for further refinement of the orientation parameters as well as for correction of the contrast transfer function (CTF). The resolution of the final density map was ~35 Å according to Fourier shell correlation (FSC) using the FSC = 0.5 criterion (Figure S6).

For the 2D analysis of the quarternary gp130/IL-6/IL-6Rα/Jak1 transmembrane complex we interactively selected 14,008 particles from 224 images taken on imaging plates (Figure S7). After a first classification into 150 groups, we selected 3975 particles from those classes that clearly resolved the receptor complex ectodomain, and subjected them to a final classification into 30 classes (Figure S8).

Molecular Modeling of Jak1

Docking, modeling, and molecular graphics for Jak1 were generated using the UCSF Chimera package from the Resource for Biocomputing, Visualization, and Informatics at the University of California, San Francisco (Pettersen et al., 2004). Due to the limited resolution of our maps (~35 Å) we only employed manual procedures to dock crystal structures into the 3D densities. To model the kinase and pseudokinase domains we used two copies of the atomic resolution structure of the Jak1 kinase domain (PDB ID: 3EYH) (Williams et al., 2009). The Jak1 FERM domain was modeled using the homologous Focal Adhesion Kinase FERM domain (PDB ID: 2AL6) (Ceccarelli et al., 2006), whereas the Jak1 SH2 domain was modeled using a Src tyrosine kinase SH2 domain (PDB ID: 1IJR) (Kawahata et al., 2001).

Preparation of gp130/IL-6/IL-6Rα Nanodiscs

Nanodiscs were prepared using standard procedures essentially as described (Ritchie et al., 2009). 1,2-Dipalmitoyl-sn-glycero-3-phosphocholine (DPPC, Avanti Polar Lipids), dried overnight in a centrifugal evaporator, was solubilized in 100 mM cholate (Na cholate hydrate, SIGMA) (end concentration of DPPC: 50 mM) and incubated with membrane scaffold protein MSP1 and gp130-hyper-IL-6 complex at 37°C for 15 min at end concentrations of 7 mM (DPPC), 18 mM (cholate), 78 μM (MSP1), and 5.6 μM (gp130-hyper-IL-6 complex), respectively. The mixture was supplemented with 0.02% (w/v) n-dodecyl-β-D-maltopyranoside, 0.2% (v/v) 2-mercaptoethanol, and 1 mM phenylmethylsulfonyl fluoride (PMSF), respectively. After the incubation period at 37°C, 475 mg wet Bio-Beads SM-2 (BIO-RAD), washed with methanol and water, were added to the sample and incubated at 4°C for 9 hr on a rotating wheel to remove the detergent and initiate nanodisc self-assembly. The sample was subsequently analyzed by gel filtration on a Superose 6 column in 10 mM HEPES (pH 7.2), 150 mM NaCl, and 0.2% (v/v) 2-mercaptoethanol. We observed highly efficient nanodisc formation, and the complex eluted on gel filtration as a monodisperse peak.

SUPPLEMENTAL INFORMATION

Supplemental Information includes eight figures and can be found with this article online at doi:10.1016/j.str.2010.10.010.

ACKNOWLEDGMENTS

We thank Stefan Rose-John for helpful discussion and gift of the hyper-IL6 cDNA. The molecular EM facility at Harvard Medical School was established with a generous donation from the Giovanni Armenise Harvard Center for Structural Biology (T.W.). P.J.L. and G.S are Damon Runyon Fellows, supported by the Damon Runyon Cancer Research Foundation (DRG-1928-06 to P.J.L. and DRG-1824-04 to G.S.). C.T. is supported by a postdoctoral fellowship of the International Human Frontier Science Program Organization. This work was funded, in part, by an NIH grant (AI51321) to K.C.G. K.C.G. and T.W. are Investigators of the Howard Hughes Medical Institute.

Received: August 9, 2010
Revised: September 25, 2010
Accepted: October 31, 2010
Published: January 11, 2011

REFERENCES

Boggon, T.J., Li, Y., Manley, P.W., and Eck, M.J. (2005). Crystal structure of the Jak3 kinase domain in complex with a staurosporine analog. Blood *106*, 996–1002.

Boulanger, M.J., and Garcia, K.C. (2004). Shared cytokine signaling receptors: structural insights from the gp130 system. Adv. Protein Chem. *68*, 107–146.

Boulanger, M.J., Bankovich, A.J., Kortemme, T., Baker, D., and Garcia, K.C. (2003a). Convergent mechanisms for recognition of divergent cytokines by the shared signaling receptor gp130. Mol. Cell *12*, 577–589.

Boulanger, M.J., Chow, D.C., Brevnova, E.E., and Garcia, K.C. (2003b). Hexameric structure and assembly of the interleukin-6/IL-6 alpha-receptor/gp130 complex. Science *300*, 2101–2104.

Bravo, J., and Heath, J.K. (2000). Receptor recognition by gp130 cytokines. EMBO J. *19*, 2399–2411.

Ceccarelli, D.F., Song, H.K., Poy, F., Schaller, M.D., and Eck, M.J. (2006). Crystal structure of the FERM domain of focal adhesion kinase. J. Biol. Chem. *281*, 252–259.

Chow, D., Ho, J., Nguyen Pham, T.L., Rose-John, S., and Garcia, K.C. (2001). In vitro reconstitution of recognition and activation complexes between interleukin-6 and gp130. Biochemistry *40*, 7593–7603.

Chrencik, J.E., Patny, A., Leung, I.K., Korniski, B., Emmons, T.L., Hall, T., Weinberg, R.A., Gormley, J.A., Williams, J.M., Day, J.E., et al. (2010). Structural and thermodynamic characterization of the TYK2 and JAK3 kinase domains in complex with CP-690550 and CMP-6. J. Mol. Biol. *400*, 413–433.

Constantinescu, S.N., Keren, T., Socolovsky, M., Nam, H., Henis, Y.I., and Lodish, H.F. (2001). Ligand-independent oligomerization of cell-surface erythropoietin receptor is mediated by the transmembrane domain. Proc. Natl. Acad. Sci. USA *98*, 4379–4384.

de Vos, A.M., Ultsch, M., and Kossiakoff, A.A. (1992). Human growth hormone and extracellular domain of its receptor: crystal structure of the complex. Science *255*, 306–312.

Dukkipati, A., Park, H.H., Waghray, D., Fischer, S., and Garcia, K.C. (2008). BacMam system for high-level expression of recombinant soluble and membrane glycoproteins for structural studies. Protein Expr. Purif. *62*, 160–170.

Fischer, M., Goldschmitt, J., Peschel, C., Brakenhoff, J.P., Kallen, K.J., Wollmer, A., Grotzinger, J., and Rose-John, S. (1997). I. A bioactive designer cytokine for human hematopoietic progenitor cell expansion. Nat. Biotechnol. *15*, 142–145.

Frank, J., Radermacher, M., Penczek, P., Zhu, J., Li, Y., Ladjadj, M., and Leith, A. (1996). SPIDER and WEB: processing and visualization of images in 3D electron microscopy and related fields. J. Struct. Biol. *116*, 190–199.

Funakoshi-Tago, M., Pelletier, S., Moritake, H., Parganas, E., and Ihle, J.N. (2008). Jak2 FERM domain interaction with the erythropoietin receptor regulates Jak2 kinase activity. Mol. Cell. Biol. *28*, 1792–1801.

Haan, C., Heinrich, P.C., and Behrmann, I. (2002). Structural requirements of the interleukin-6 signal transducer gp130 for its interaction with Janus kinase 1: the receptor is crucial for kinase activation. Biochem. J. *361*, 105–111.

Haan, C., Kreis, S., Margue, C., and Behrmann, I. (2006). Jaks and cytokine receptors—an intimate relationship. Biochem. Pharmacol. *72*, 1538–1546.

Heinrich, P.C., Behrmann, I., Haan, S., Hermanns, H.M., Muller-Newen, G., and Schaper, F. (2003). Principles of interleukin (IL)-6-type cytokine signalling and its regulation. Biochem. J. *374*, 1–20.

Ihle, J.N. (1995). Cytokine receptor signalling. Nature *377*, 591–594.

Kawahata, N., Yang, M.G., Luke, G.P., Shakespeare, W.C., Sundaramoorthi, R., Wang, Y., Johnson, D., Merry, T., Violette, S., Guan, W., et al. (2001). A novel phosphotyrosine mimetic 4′-carboxymethyloxy-3′-phosphonophenylalanine (Cpp): exploitation in the design of nonpeptide inhibitors of pp60(Src) SH2 domain. Bioorg. Med. Chem. Lett. *11*, 2319–2323.

Kubatzky, K.F., Ruan, W., Gurezka, R., Cohen, J., Ketteler, R., Watowich, S.S., Neumann, D., Langosch, D., and Klingmuller, U. (2001). Self assembly of the transmembrane domain promotes signal transduction through the erythropoietin receptor. Curr. Biol. *11*, 110–115.

Kurth, I., Horsten, U., Pflanz, S., Timmermann, A., Kuster, A., Dahmen, H., Tacken, I., Heinrich, P.C., and Muller-Newen, G. (2000). Importance of the membrane-proximal extracellular domains for activation of the signal transducer glycoprotein 130. J. Immunol. *164*, 273–282.

Leonard, W.J., and O'Shea, J.J. (1998). Jaks and STATs: biological implications. Annu. Rev. Immunol. *16*, 293–322.

Lietha, D., Cai, X., Ceccarelli, D.F., Li, Y., Schaller, M.D., and Eck, M.J. (2007). Structural basis for the autoinhibition of focal adhesion kinase. Cell *129*, 1177–1187.

Lindauer, K., Loerting, T., Liedl, K.R., and Kroemer, R.T. (2001). Prediction of the structure of human Janus kinase 2 (JAK2) comprising the two carboxy-terminal domains reveals a mechanism for autoregulation. Protein Eng. *14*, 27–37.

Lucet, I.S., Fantino, E., Styles, M., Bamert, R., Patel, O., Broughton, S.E., Walter, M., Burns, C.J., Treutlein, H., Wilks, A.F., and Rossjohn, J. (2006). The structural basis of Janus kinase 2 inhibition by a potent and specific pan-Janus kinase inhibitor. Blood *107*, 176–183.

Matadeen, R., Hon, W.C., Heath, J.K., Jones, E.Y., and Fuller, S. (2007). The dynamics of signal triggering in a gp130-receptor complex. Structure *15*, 441–448.

Murakami, M., Narazaki, M., Hibi, M., Yawata, H., Yasukawa, K., Hamaguchi, K., Taga, T., and Kishimoto, T. (1991). Critical cytoplasmic region of the interleukin-6 signal transducer gp130 is conserved in the cytokine receptor family. Proc. Natl. Acad. Sci. USA *88*, 11349–11353.

Ohi, M., Li, Y., Cheng, Y., and Walz, T. (2004). Negative staining and image classification—powerful tools in modern electron microscopy. Biol. Proced. Online *6*, 23–34.

Pettersen, E.F., Goddard, T.D., Huang, C.C., Couch, G.S., Greenblatt, D.M., Meng, E.C., and Ferrin, T.E. (2004). UCSF Chimera–a visualization system for exploratory research and analysis. J. Comput. Chem. *25*, 1605–1612.

Radermacher, M., Wagenknecht, T., Verschoor, A., and Frank, J. (1987). Three-dimensional reconstruction from a single-exposure, random conical tilt series applied to the 50S ribosomal subunit of Escherichia coli. J. Microsc. *146*, 113–136.

Ritchie, T.K., Grinkova, Y.V., Bayburt, T.H., Denisov, I.G., Zolnerciks, J.K., Atkins, W.M., and Sligar, S.G. (2009). Chapter 11 - Reconstitution of membrane proteins in phospholipid bilayer nanodiscs. Methods Enzymol. *464*, 211–231.

Saharinen, P., and Silvennoinen, O. (2002). The pseudokinase domain is required for suppression of basal activity of Jak2 and Jak3 tyrosine kinases and for cytokine-inducible activation of signal transduction. J. Biol. Chem. *277*, 47954–47963.

Schindler, C., Levy, D.E., and Decker, T. (2007). JAK-STAT signaling: from interferons to cytokines. J. Biol. Chem. *282*, 20059–20063.

Seubert, N., Royer, Y., Staerk, J., Kubatzky, K.F., Moucadel, V., Krishnakumar, S., Smith, S.O., and Constantinescu, S.N. (2003). Active and inactive orientations of the transmembrane and cytosolic domains of the erythropoietin receptor dimer. Mol. Cell *12*, 1239–1250.

Skiniotis, G., Boulanger, M.J., Garcia, K.C., and Walz, T. (2005). Signaling conformations of the tall cytokine receptor gp130 when in complex with IL-6 and IL-6 receptor. Nat. Struct. Mol. Biol. *12*, 545–551.

Skiniotis, G., Lupardus, P.J., Martick, M., Walz, T., and Garcia, K.C. (2008). Structural organization of a full-length gp130/LIF-R cytokine receptor transmembrane complex. Mol. Cell *31*, 737–748.

Stewart, A., and Grigorieff, N. (2004). Noise bias in the refinement of structures derived from single particles. Ultramicroscopy *102*, 67–84.

Stroud, R.M., and Wells, J.A. (2004). Mechanistic diversity of cytokine receptor signaling across cell membranes. Sci. STKE *2004*, re7.

Wang, X., Lupardus, P., Laporte, S.L., and Garcia, K.C. (2009). Structural biology of shared cytokine receptors. Annu. Rev. Immunol. *27*, 29–60.

Williams, N.K., Bamert, R.S., Patel, O., Wang, C., Walden, P.M., Wilks, A.F., Fantino, E., Rossjohn, J., and Lucet, I.S. (2009). Dissecting specificity in the Janus kinases: the structures of JAK-specific inhibitors complexed to the JAK1 and JAK2 protein tyrosine kinase domains. J. Mol. Biol. *387*, 219–232.

Xu, Y., Kershaw, N.J., Luo, C.S., Soo, P., Pocock, M.J., Czabotar, P.E., Hilton, D.J., Nicola, N.A., Garrett, T.P., and Zhang, J.G. (2010). Crystal structure of the entire ectodomain of GP130: insights into the molecular assembly of the tall cytokine receptor complexes. J. Biol. Chem. *285*, 21214–21218.

Zhou, Y.J., Chen, M., Cusack, N.A., Kimmel, L.H., Magnuson, K.S., Boyd, J.G., Lin, W., Roberts, J.L., Lengi, A., Buckley, R.H., et al. (2001). Unexpected effects of FERM domain mutations on catalytic activity of Jak3: structural implication for Janus kinases. Mol. Cell *8*, 959–969.